



Organic peroxy radical chemistry in oxidation flow reactors and environmental chambers and their atmospheric relevance

Zhe Peng¹, Julia Lee-Taylor^{1,2}, John J. Orlando², Geoffrey S. Tyndall², and Jose L. Jimenez¹

¹Cooperative Institute for Research in Environmental Sciences and Department of Chemistry, University of Colorado, Boulder, Colorado 80309, USA

²Atmospheric Chemistry Observation and Modeling Laboratory, National Center for Atmospheric Research, Boulder, Colorado 80307, USA

Correspondence: Zhe Peng (zhe.peng@colorado.edu) and Jose L. Jimenez (jose.jimenez@colorado.edu)

Received: 9 September 2018 – Discussion started: 24 September 2018

Revised: 16 December 2018 – Accepted: 8 January 2019 – Published: 22 January 2019

Abstract. Oxidation flow reactors (OFRs) are a promising complement to environmental chambers for investigating atmospheric oxidation processes and secondary aerosol formation. However, questions have been raised about how representative the chemistry within OFRs is of that in the troposphere. We investigate the fates of organic peroxy radicals (RO_2), which play a central role in atmospheric organic chemistry, in OFRs and environmental chambers by chemical kinetic modeling and compare to a variety of ambient conditions to help define a range of atmospherically relevant OFR operating conditions. For most types of RO_2 , their bimolecular fates in OFRs are mainly $\text{RO}_2 + \text{HO}_2$ and $\text{RO}_2 + \text{NO}$, similar to chambers and atmospheric studies. For substituted primary RO_2 and acyl RO_2 , $\text{RO}_2 + \text{RO}_2$ can make a significant contribution to the fate of RO_2 in OFRs, chambers and the atmosphere, but $\text{RO}_2 + \text{RO}_2$ in OFRs is in general somewhat less important than in the atmosphere. At high NO, $\text{RO}_2 + \text{NO}$ dominates RO_2 fate in OFRs, as in the atmosphere. At a high UV lamp setting in OFRs, $\text{RO}_2 + \text{OH}$ can be a major RO_2 fate and RO_2 isomerization can be negligible for common multifunctional RO_2 , both of which deviate from common atmospheric conditions. In the OFR254 operation mode (for which OH is generated only from the photolysis of added O_3), we cannot identify any conditions that can simultaneously avoid significant organic photolysis at 254 nm and lead to RO_2 lifetimes long enough (~ 10 s) to allow atmospherically relevant RO_2 isomerization. In the OFR185 mode (for which OH is generated from reactions initiated by 185 nm photons), high relative humidity, low UV intensity and low precursor concentrations are recom-

mended for the atmospherically relevant gas-phase chemistry of both stable species and RO_2 . These conditions ensure minor or negligible $\text{RO}_2 + \text{OH}$ and a relative importance of RO_2 isomerization in RO_2 fate in OFRs within $\sim \times 2$ of that in the atmosphere. Under these conditions, the photochemical age within OFR185 systems can reach a few equivalent days at most, encompassing the typical ages for maximum secondary organic aerosol (SOA) production. A small increase in OFR temperature may allow the relative importance of RO_2 isomerization to approach the ambient values. To study the heterogeneous oxidation of SOA formed under atmospherically relevant OFR conditions, a different UV source with higher intensity is needed after the SOA formation stage, which can be done with another reactor in series. Finally, we recommend evaluating the atmospheric relevance of RO_2 chemistry by always reporting measured and/or estimated OH, HO_2 , NO, NO_2 and OH reactivity (or at least precursor composition and concentration) in all chamber and flow reactor experiments. An easy-to-use RO_2 fate estimator program is included with this paper to facilitate the investigation of this topic in future studies.

1 Introduction

Laboratory reactors are needed to isolate and study atmospheric chemical systems. Environmental chambers have been a major atmospheric chemistry research tool for decades (Cocker et al., 2001; Carter et al., 2005; Presto et al., 2005; Wang et al., 2011; Platt et al., 2013). Over the last

few years, oxidation flow reactors (OFRs; see Appendix A for the meanings of the acronyms) (Kang et al., 2007) have emerged as a promising complement to chambers and are being used to investigate atmospheric oxidation processes, particularly volatile organic compound (VOC) oxidation and secondary organic aerosol (SOA) formation and aging (Kang et al., 2011; Lambe et al., 2015; Hu et al., 2016; Palm et al., 2016). These processes have air quality (Levy II, 1971), human health (Nel, 2005) and climate impacts (Stocker et al., 2014).

The most important advantage of OFRs is their ability to achieve relatively high photochemical ages (of the order of equivalent hours or days assuming an average ambient OH concentration of 1.5×10^6 molecules cm^{-3} ; Mao et al., 2009) in minutes instead of hours in chambers (Lambe et al., 2011). Rapid aging is usually achieved by highly active HO_x radical chemistry initiated by low-pressure Hg lamp emissions (185 and 254 nm) (Li et al., 2015; Peng et al., 2015). This allows for shorter residence times in OFRs, thus reducing the relative importance of gas and particle losses to walls (Palm et al., 2016), which can be very important in Teflon chambers (Cocker et al., 2001; Matsunaga and Ziemann, 2010; Zhang et al., 2014; Krechmer et al., 2016). In addition, the lower costs and small size (volumes of the order of 10 L) of OFRs allow for better portability. These, together with the ability to rapidly achieve high photochemical ages, are advantageous for field applications. These advantages of OFRs have led a number of atmospheric chemistry research groups (Lambe and Jimenez, 2018) to deploy them in field (Hu et al., 2016; Ortega et al., 2016; Palm et al., 2016, 2017), source (Ortega et al., 2013; Tkacik et al., 2014; Karjalainen et al., 2016; Link et al., 2016) and laboratory studies (Kang et al., 2011; Lambe et al., 2013; Richards-Henderson et al., 2016; Lim et al., 2017).

While the use of oxidation flow reactors is growing rapidly in the atmospheric chemistry community, some researchers have raised two concerns with regard to OFRs: (1) the chemical regime of OFRs may be unrealistic compared to the atmosphere, and (2) OFRs are derivative of flow reactors with a long tradition in atmospheric chemistry, especially for chemical kinetic measurements, and thus there is not much new to be discussed or analyzed in their chemistry. While it is true that OFRs follow the tradition of flow tubes used in atmospheric chemistry, they attempt to simulate a much more complex system all at once and typically use much longer residence times, and thus many fundamental and practical issues arise that have not been addressed before. The need to achieve longer effective photochemical ages within a short residence time can, however, lead to the occurrence of undesirable oxidation pathways.

To clarify this issue, a series of chemical kinetic modeling studies have been performed: Li et al. (2015) and Peng et al. (2015) established a radical chemistry and oxidation model whose predictions compare well against laboratory experiments and found that OH can be substantially sup-

pressed by external OH reactants (e.g., SO_2 , NO_x and VOCs externally introduced into the reactor); Peng et al. (2016) identified a low water mixing ratio (H_2O) and/or high external OH reactivity (OHR_{ext} , i.e., first-order OH loss rate constant contributed by external OH reactants) as conditions that can cause significant non-tropospheric VOC reactions (e.g., through photolysis at 185 and/or 254 nm); Peng and Jimenez (2017) studied NO_y chemistry in OFRs and showed that high-NO conditions, under which organic peroxy radicals react more rapidly with NO than with HO_2 , can only be realized by simple NO injection in a very narrow range of physical conditions, whose application to investigating intermediate- and high-NO environments (e.g., urban area) is limited; Peng et al. (2018) thus evaluated a few new techniques to maintain high-NO conditions in OFRs and found the injection of percent-level N_2O effective to achieve this goal.

While HO_x and NO_y chemistries have been extensively characterized in OFRs so far, organic peroxy radical (RO_2) chemistry has yet to be considered in detail, as previous studies have only considered the balance between $\text{RO}_2 + \text{NO}$ vs. $\text{RO}_2 + \text{HO}_2$. There has been some speculation that due to high OH concentrations in OFRs, RO_2 concentration and lifetime might be significantly different from ambient values, leading to the dominance of RO_2 self- and cross-reactions and the elimination of RO_2 isomerization pathways (Crouse et al., 2013; Praske et al., 2018). Given the central role RO_2 plays in atmospheric chemistry (Orlando and Tyndall, 2012; Ziemann and Atkinson, 2012) and the rapidly increasing use of OFRs, RO_2 chemistry in OFRs needs to be studied in detail to characterize the similarities and differences between their reaction conditions and those in the ambient atmosphere and traditional atmospheric reaction chambers.

In this paper, we address this need via modeling. All major known fates of RO_2 in OFRs will be investigated and compared with those in typical chamber cases and in the atmosphere. This comparison will provide insights into the atmospheric relevance of RO_2 chemistry in atmospheric simulation reactors and allow for the selection of experimental conditions with atmospherically relevant RO_2 chemistry in experimental planning.

2 Methods

Due to a variety of loss pathways of RO_2 and a myriad of RO_2 types, RO_2 chemistry is of enormous complexity. We detail the RO_2 production and loss pathways of interest in this study, the approximations used to simplify this complex problem and the steps to investigate it methodically. We briefly introduce the base OFR design and the model, which are described in detail elsewhere (Kang et al., 2007; Peng et al., 2015, 2018).

2.1 Potential aerosol mass oxidation flow reactor (PAM OFR)

The concept of the base OFR design simulated in this study, the potential aerosol mass (PAM) reactor, was first introduced by Kang et al. (2007). The geometry of the most popular PAM OFR is a cylinder of ~ 13 L volume. The PAM reactor we simulate is equipped with low-pressure Hg lamps (model no. 82-9304-03, BHK Inc.) emitting UV light at 185 and 254 nm. When both 185 and 254 nm photons are used to generate OH (termed “OFR185”), water vapor photolysis at 185 nm produces OH and HO₂. Recombination of O₂ and O(³P), formed by O₂ photolysis at 185 nm, generates O₃. O(¹D), formed through O₃ photolysis at 254 nm, reacts with water vapor and produces additional OH. 185 nm photons can be filtered by installing quartz sleeves around the lamps. This converts the reactor into “OFR254” mode, for which the photolysis of O₃, which must be initially injected, is the only OH production route. The notation “OFR254-X” is used to specify the initial amount of injected O₃ (*X* ppm) in OFR254. Lambe et al. (2017) and Peng et al. (2018) have shown that the initial injection of N₂O is able to maintain up to tens of ppb NO in both OFR185 and OFR254. These modes are denoted “OFR185-iN₂O” and “OFR254-X-iN₂O”, or more generally “OFR-iN₂O”. In OFR254-iN₂O, O(¹D) generated from O₃ photolysis reacts with N₂O to generate NO, while in OFR185-iN₂O, O(¹D) is mainly supplied by N₂O photolysis at 185 nm (Peng et al., 2018).

2.2 RO₂ production and loss pathways

A single generic RO₂ is adopted for modeling purposes to avoid the huge number of RO₂ types that would complicate effective modeling and analysis. In OH-initiated VOC oxidation, RO₂ is primarily produced via VOC + OH → R (+H₂O) followed by R + O₂ → RO₂, where R is hydrocarbyl or oxygenated hydrocarbyl radical. Since the second step is extremely fast in air (Atkinson and Arey, 2003), the first step controls the RO₂ production rate, which depends on OH concentration and OHR_{ext} due to VOCs (OHR_{VOC}; see Appendix B for details). OHR_{VOC} also includes the contribution from oxidation intermediates of primary VOCs (e.g., methyl vinyl ketone and pinonic acid). When the information about oxidation intermediates is insufficient to calculate OHR_{VOC}, OHR due to primary VOCs is used instead as an approximant. RO₂ production through other pathways, e.g., VOC ozonolysis and photolysis, is not considered, since all non-OH pathways of VOC destruction only become significant at low H₂O and/or high OHR_{ext} (Peng et al., 2016). These conditions lead to significant non-tropospheric VOC photolysis and thus are of little experimental interest.

Table 1 lists all known RO₂ loss pathways. Among those, RO₂ photolysis, RO₂ + NO₃ and RO₂ + O₃ are not included in this study, since they are minor or negligible in OH-

dominated atmospheres, chambers and OFRs for the following reasons.

The first-order RO₂ photolysis rate constant is of the order of 10^{-2} s⁻¹ at the highest lamp setting in OFRs (Kalafut-Pettibone et al., 2013) and of the order of 10^{-5} s⁻¹ in the troposphere under the assumption of unity quantum yield (Klems et al., 2015), while RO₂ reacts with HO₂ at > 1 s⁻¹ at the highest lamp setting in OFRs and at $\sim 2 \times 10^{-3}$ s⁻¹ in the troposphere. Note that in this study we assume an average ambient HO₂ concentration of 1.5×10^8 molecules cm⁻³ (Mao et al., 2009; Stone et al., 2012) and RO₂ + HO₂ rate constant of 1.5×10^{-11} cm³ molecule⁻¹ s⁻¹ (Orlando and Tyndall, 2012).

When daytime photochemistry is active, NO₃ is negligible in the atmosphere. In OFR-iN₂O modes, RO₂ + NO₃ is negligible unless at very low H₂O and high UV intensity (abbreviated UV hereafter), which result in high O₃ to oxidize NO₂ to NO₃ and keep HO₂ minimized. However, very low H₂O causes serious non-tropospheric organic photolysis (Peng et al., 2016) and thus these conditions are of no experimental interest.

In the atmosphere RO₂ + O₃ is thought to play some role only at night (Orlando and Tyndall, 2012). Similar conditions may exist in some OFR254 cases if a very large amount of O₃ is injected and H₂O and UV are kept very low to limit HO_x production. These conditions are obviously not OH dominated and not further investigated in this study.

Of the RO₂ fates considered in this study, RO₂ + HO₂, RO₂ + NO and RO₂ + RO₂ have long been known to play a role in the atmosphere (Orlando and Tyndall, 2012). Recommended general rate constants are available for RO₂ + HO₂ and RO₂ + NO (Ziemann and Atkinson, 2012; Table 1), albeit with some small dependencies on the type of RO₂ and a few deviations that are slightly larger but not important for the overall chemistry (e.g., CH₃O₂ and C₂H₅O₂ for RO₂ + HO₂). We use these recommended values for generic RO₂ in this study. RO₂ + NO has two main product channels, i.e., RO + NO₂ and RONO₂, whose branching ratios are RO₂ structure dependent (Ziemann and Atkinson, 2012). We do not include these product channels in this study, since they have negligible impacts on the chemical scheme described here. This feature results from two facts: (i) we focus on generic RO₂ and do not explicitly consider the chemistry of the products of different RO₂ loss pathways; and (ii) the channel producing RO and NO₂ contributes little to NO₂ production (Peng et al., 2018). However, RO₂ self- and cross-reaction rate constants are highly dependent on the specific RO₂ types and can vary over a very large range (10^{-17} – 10^{-10} cm³ molecule⁻¹ s⁻¹). Unsubstituted primary, secondary and tertiary RO₂ radicals self-react at $\sim 10^{-13}$, $\sim 10^{-15}$ and $\sim 10^{-17}$ cm³ molecule⁻¹ s⁻¹, respectively (Ziemann and Atkinson, 2012). Rate constants of cross-reactions between these RO₂ types also span this range (Orlando and Tyndall, 2012). Substituted RO₂ types have higher self- and cross-reaction rate constants (Orlando

Table 1. Rate constants (in $\text{cm}^3 \text{ molecule}^{-1} \text{ s}^{-1}$ except for isomerization; in s^{-1}), cross section (in cm^2) and product(s) of RO_2 loss pathways. Only organic species are listed for product(s).

RO_2 loss pathway	Rate constant or cross section	Product(s)
$\text{RO}_2 + \text{HO}_2$	1.5×10^{-11} ^a	mainly ROOH for most RO_2 ^a
$\text{RO}_2 + \text{NO}$	9×10^{-12} ^a	RO , RONO_2 ^b
$\text{RO}_2 + \text{RO}_2$	Primary: $\sim 10^{-13}$ ^a Secondary: $\sim 10^{-15}$ ^a Tertiary: $\sim 10^{-17}$ ^a Substituted: can be up to 2 orders of magnitude higher ^b Acyl: $\sim 10^{-11}$ ^b	$\text{ROH} + \text{R(=O)}$, $\text{RO} + \text{RO}$, ROOR ^a
$\text{RO}_2 + \text{NO}_2$ (in OFRs)	7×10^{-12} ^c	RO_2NO_2 ^b
$\text{RO}_2 + \text{OH}$	1×10^{-10} ^d	ROOOH (for $\geq \text{C}_4 \text{ RO}_2$), RO (smaller RO_2) ^e
RO_2 isomerization	Autoxidation: $\sim 10^{-3}$ – 10^{2f} Other: up to 10^{6g}	generally another RO_2
RO_2 photolysis	$\sim 10^{-18}$ at 254 nm ^h $\sim 10^{-21}$ – 10^{-19} in UVA and UVB ^h	mainly R , other photochemical products possible ⁱ
$\text{RO}_2 + \text{NO}_3$	~ 1 – 3×10^{-12} ^b	RO^b
$\text{RO}_2 + \text{O}_3$	$\sim 10^{-17}$ ^b	RO^b

^a Ziemann and Atkinson (2012). ^b Orlando and Tyndall (2012); ^c typical value within the reported range in Orlando and Tyndall (2012); thermal decomposition rate constants of nitrates of acyl and non-acyl RO_2 are assumed to be 0.0004 and 3 s^{-1} , respectively, which are also typical values within the reported ranges in Orlando and Tyndall (2012). ^d Value used in the present work based on Bossolasco et al. (2014); Assaf et al. (2016, 2017a); Müller et al. (2016); Yan et al. (2016). ^e Müller et al. (2016); Yan et al. (2016); Assaf et al. (2017b, 2018). ^f Crouse et al. (2013). ^g Knap and Jørgensen (2017). ^h Burkholder et al. (2015). ⁱ Klems et al. (2015).

and Tyndall, 2012). $\text{RO}_2 + \text{RO}_2$ of highly substituted primary RO_2 can be as high as $\sim 10^{-11} \text{ cm}^3 \text{ molecule}^{-1} \text{ s}^{-1}$ (Orlando and Tyndall, 2012). Very recently, a few highly oxidized 1,3,5-trimethylbenzene-derived RO_2 s were reported to self- and cross-react at $\sim 10^{-10} \text{ cm}^3 \text{ molecule}^{-1} \text{ s}^{-1}$ (Berndt et al., 2018). In the present work, we make a simplification to adapt to the generic RO_2 treatment by assuming a single self- and cross-reaction rate constant for generic RO_2 in each case. Three levels of $\text{RO}_2 + \text{RO}_2$ rate constants, i.e., 1×10^{-13} , 1×10^{-11} and $1 \times 10^{-10} \text{ cm}^3 \text{ molecule}^{-1} \text{ s}^{-1}$, are studied in this paper. The first level is referred to as “medium $\text{RO}_2 + \text{RO}_2$ ” as many other RO_2 types can have self- and cross-reaction rate constants as low as $10^{-17} \text{ cm}^3 \text{ molecule}^{-1} \text{ s}^{-1}$; the second level is defined as “fast $\text{RO}_2 + \text{RO}_2$ ”; and the last level is called “very fast $\text{RO}_2 + \text{RO}_2$ ”. No $\text{RO}_2 + \text{RO}_2$ rate constant lower than the medium level is investigated in the current work, although there are still a large variety of RO_2 types whose self- and cross-reactions are at lower rate constants, since at the medium level, $\text{RO}_2 + \text{RO}_2$ is already negligible in all the environments studied in this work, i.e., OFRs, chambers and the atmosphere (see Sect. 3.1.1). Since there are only a few very specific examples for very fast $\text{RO}_2 + \text{RO}_2$ reported to date, we will not systematically explore this category but compare very fast $\text{RO}_2 + \text{RO}_2$ as a sensitivity case with the other two types of $\text{RO}_2 + \text{RO}_2$ reactions.

Acyl RO_2 is considered as a separate RO_2 type (neither medium nor fast $\text{RO}_2 + \text{RO}_2$) in this study since its reaction with NO_2 can be a major sink of RO_2 in OFR

(Peng and Jimenez, 2017). Thermal decomposition lifetimes of the product of $\text{RO}_2 + \text{NO}_2$, i.e., acylperoxy nitrates, can be hours at laboratory temperatures (Orlando and Tyndall, 2012; also taken into account in the current work; see Table 1), while OFR residence times are typically minutes. Besides, acyl RO_2 reacts with many RO_2 types at $\sim 10^{-11} \text{ cm}^3 \text{ molecule}^{-1} \text{ s}^{-1}$ (Orlando and Tyndall, 2012), similar to that of fast $\text{RO}_2 + \text{RO}_2$. We thus assume the acyl RO_2 self- and cross-reaction rate constant to also be $1 \times 10^{-11} \text{ cm}^3 \text{ molecule}^{-1} \text{ s}^{-1}$ to facilitate comparison with fast $\text{RO}_2 + \text{RO}_2$ results.

In OFRs operated at room temperature, acylperoxy nitrates barely decompose, as their thermal decomposition lifetime is typically $\sim 1 \text{ h}$ (Orlando and Tyndall, 2012), while OFR residence time is usually a few minutes. In contrast, peroxy nitrates of non-acyl RO_2 do decompose on a timescale of 0.1 s (Orlando and Tyndall, 2012; Table 1). As a consequence, the production and decomposition of peroxy nitrates of non-acyl RO_2 reach a steady state in OFRs, which can be greatly shifted toward the peroxy nitrate side in cases with very high NO_2 (Peng and Jimenez, 2017; Peng et al., 2018).

$\text{RO}_2 + \text{OH}$ (Fittschen et al., 2014) and RO_2 isomerization (Crouse et al., 2013) have recently been identified as possible significant RO_2 fates in the atmosphere. Reactions of the former type, according to several recent experimental and theoretical studies (Bossolasco et al., 2014; Assaf et al., 2016, 2017a, b; Müller et al., 2016; Yan et al., 2016), have similar rate constants ($\sim 1 \times$

$10^{-10} \text{ cm}^3 \text{ molecule}^{-1} \text{ s}^{-1}$) regardless of RO_2 type. Therefore, the reaction rate constant of generic RO_2 with OH is assigned as $1 \times 10^{-10} \text{ cm}^3 \text{ molecule}^{-1} \text{ s}^{-1}$. RO_2 isomerization reactivity is highly structure dependent (Crouse et al., 2013; Praske et al., 2018) and rate constant measurements are still scarce, preventing us from assigning a generic RO_2 isomerization rate constant. However, for *generic* RO_2 , isomerization is generally *not* a sink but a conversion between two RO_2 radicals (both encompassed by the generic one in this study), as RO_2 isomerization usually generates an oxygenated hydrocarbyl radical, which rapidly recombines with O_2 and forms another RO_2 . Therefore, RO_2 isomerization is not explicitly taken into account in the modeling, but is considered in the RO_2 fate analysis.

In summary, six pathways are included in the RO_2 fate analysis of this study. The need to explore these six pathways for a high number of OFR, chamber and atmospheric conditions makes the presentation of results challenging. For clarity, we present the results in two steps. In the first step, only well-known RO_2 fates (reaction with NO_2 , HO_2 , NO and RO_2) will be included in the model. In the second step, the results of the first step will be used to guide the modeling and analysis of a more comprehensive set of significant RO_2 fates.

2.3 Model description

The model used in the present work is a standard chemical kinetic box model implemented in the KinSim 3.4 solver in Igor Pro 7 (WaveMetrics, Lake Oswego, Oregon, USA) and has been described in detail elsewhere (Peng et al., 2015, 2018). Plug flow in the reactor with a residence time of 180 s is assumed, since the effects of non-plug flow are major only in a narrow range of conditions of little experimental interest, and the implementation of laminar flow or measured residence time distribution substantially increases computational cost (Peng et al., 2015; Peng and Jimenez, 2017). The reactions of RO_2 discussed in Sect. 2.2 are added to the chemical mechanism. A generic slow-reacting VOC (with the same OH rate constant as SO_2) is used as the external OH reactant. Its initial concentration is determined by the initial OHR_{ext} in each model case. Then as this proxy external OH reactant slowly reacts, OHR_{ext} slowly decays. This slow change in OHR_{ext} represents not only the decay of the initial reactant but also the generation and consumption of later-generation products that continue to react with OH. The reason for this approximation has been discussed in detail in previous OFR modeling papers (Peng and Jimenez, 2017; Peng et al., 2018). We exclude NO_y species, which are explicitly modeled, from the calculation of OHR_{ext} ; thus, OHR_{ext} only includes non- NO_y OHR_{ext} hereafter. As OHR_{ext} is dominated by OHR_{VOC} in most OFR experiments, we use OHR_{ext} to denote OHR_{VOC} in OFRs (while for ambient and chamber cases OHR_{VOC} is still used to exclude the contribution of CO, etc.). The outputs of our model (e.g., species concentrations

and exposures) were estimated to be accurate to within a factor of 2–3 when compared with field OFR experiments; better agreement can generally be obtained for laboratory OFR experiments (Li et al., 2015; Peng et al., 2015).

Another key parameter in the model is the HO_x recycling ratio (β), defined in this study as the number of HO_2 molecule(s) produced per OH molecule destroyed by external OH reactants (Peng et al., 2015). This ratio depends on the products of RO_2 loss pathways. The main product of $\text{RO}_2 + \text{HO}_2$ is usually ROOH (Table 1), yielding no recycled HO_2 , while the main products of $\text{RO}_2 + \text{NO}$ are RO and NO_2 , the former of which can often undergo extremely fast H abstraction by O_2 to form a carbonyl and HO_2 . We used the fully chemically explicit (automated chemical mechanism generation based on available knowledge) box model GECKO-A (Aumont et al., 2005) to simulate OH oxidation of several simple VOCs (e.g., propane and decane) under various OFR conditions with zero NO. We consistently find that $\beta \sim 0.3$. At the other extreme, when RO_2 is solely consumed by $\text{RO}_2 + \text{NO}$, the product RO yields HO_2 at a branching ratio close to 1, $\beta \sim 1$. For intermediate cases, we assume that β may be interpolated as a linear function of $r(\text{RO}_2 + \text{NO})/[r(\text{RO}_2 + \text{NO}) + r(\text{RO}_2 + \text{HO}_2)]$, where $r(\text{RO}_2 + \text{NO})$ and $r(\text{RO}_2 + \text{HO}_2)$ are the local reactive fluxes of $\text{RO}_2 + \text{NO}$ and $\text{RO}_2 + \text{HO}_2$.

In the present work, we model OFR185, OFR254-70 and OFR254-7 (including their iN_2O variants). We specify the same temperature and atmospheric pressure (295 K and 835 mbar, typical values in Boulder, Colorado, USA) as our previous OFR modeling studies (Li et al., 2015; Peng et al., 2015, 2016, 2018; Peng and Jimenez, 2017). The explored physical condition space follows that of our previous OFR- iN_2O modeling work (Peng et al., 2018). The only differences are that in this study we also include cases without any N_2O injected (OFR185 and OFR254 only) and exclude $\text{OHR}_{\text{ext}} = 0$ conditions, which produce no RO_2 . In detail, the explored physical condition space covers the following: H_2O of 0.07%–2.3% (relative humidity of 2%–71% at 295 K); UV photon flux at 185 nm (abbreviated F185) of 1.0×10^{11} – $1.0 \times 10^{14} \text{ photons cm}^{-2} \text{ s}^{-1}$ (corresponding photon flux at 254 nm (F254) of 4.2×10^{13} – $8.5 \times 10^{15} \text{ photons cm}^{-2} \text{ s}^{-1}$); OHR_{ext} of 1–1000 s^{-1} ; and N_2O mixing ratio (abbreviated N_2O hereafter) of 0 and 0.02%–20%. All model cases are logarithmically evenly distributed except for $\text{N}_2\text{O} = 0$ and F254. The latter is calculated based on the F185–F254 relationship for the lamps simulated here (Li et al., 2015).

For the classification of conditions, the same criteria as in the OFR- iN_2O modeling study (Peng et al., 2018) are adopted. In detail, high- and low-NO conditions are classified by $r(\text{RO}_2 + \text{NO})/r(\text{RO}_2 + \text{HO}_2)$. In the current work, these reactive fluxes are explicitly tracked in the modeling instead of approximated as in previous studies (Peng and Jimenez, 2017; Peng et al., 2018). The terms “good,” “risky” and “bad” are used to describe OFR operating conditions in terms of non-tropospheric organic photolysis and are defined

based on the ratios of F185 and F254 exposure ($F_{185_{\text{exp}}}$ and $F_{254_{\text{exp}}}$, i.e., integrated photon fluxes over residence time) to OH exposure (OH_{exp}), as presented previously (Peng and Jimenez, 2017; Peng et al., 2018). Briefly, under a given condition non-tropospheric photolysis is of different relative importance in the fate of each specific organic species: under good conditions, photolysis at 185 and/or 254 nm is unimportant for almost all VOCs; under bad conditions, non-tropospheric photolysis is problematic for most VOC precursors, since significant photolysis of their oxidation intermediates at 185 and/or 254 nm is almost inevitable; and risky conditions can be problematic for some but not all VOCs. Note that good, risky or bad conditions refer only to non-tropospheric organic photolysis and *not* to whether RO_2 chemistry is atmospherically relevant. Table S1 summarizes our condition classification criteria.

3 Results and discussion

In this section, the results are presented in two parts, i.e., first for the simulations with well-known pathways only and secondly with all significant pathways, as proposed in Sect. 2.2. Then based on the results and their comparison with the atmosphere and chamber experiments, we propose guidelines for OFR operation to ensure atmospherically relevant RO_2 chemistry, as well as other chemistries already discussed in the previous studies (Peng et al., 2016, 2018), in OFRs.

3.1 Simulations with well-known pathways ($RO_2 + HO_2$, $RO_2 + RO_2$, $RO_2 + NO$ and $RO_2 + NO_2$)

Due to the significantly different reactivities of non-acyl and acyl RO_2 , the results of these two types of RO_2 are shown separately.

3.1.1 Non-acyl RO_2

In this case non-acyl RO_2 radicals have only three fates, i.e., $RO_2 + HO_2$, $RO_2 + NO$ and $RO_2 + RO_2$. The relative importance of these three fates can be shown in a triangle plot (Fig. 1). The figure includes data points of OFR185 (including OFR185- iN_2O) and OFR254-70 (including OFR254-70- iN_2O), as well as several typical ambient and chamber studies, including two pristine remote area cases (P_1 and P_2) from the ATom-1 study (Wofsy et al., 2018), two forested area cases (F_1 and F_2) from the BEACHON-RoMBAS and GoAmazon campaigns, respectively (Ortega et al., 2014; Martin et al., 2016, 2017), an urban area case (U) from the CalNex-LA campaign (Ryerson et al., 2013), and five typical chamber experiment cases (C_1 – C_5) from the FIXCIT study (Nguyen et al., 2014). These typical cases shown in Fig. 1 bring to light several interesting points.

- In all ambient and chamber cases, medium and slower $RO_2 + RO_2$ contribute negligibly to the RO_2 fate. This

confirms a common impression that self- and cross-reactions of many RO_2 radicals do not significantly affect RO_2 fates.

- However, if RO_2 self- and cross-reacts rapidly, $RO_2 + RO_2$ can be the most important loss pathway among $RO_2 + RO_2$, $RO_2 + HO_2$ and $RO_2 + NO$ even in pristine regions with higher VOC (e.g., P_1 in Fig. 1) compared to an average pristine region case (P_2). Note that the P_1 case is still very clean compared to typical forested and urban areas (Table 2).
- Forested areas located in the same region as pollution sources are not as “low NO” as one may expect (points F_1 and F_2 in Fig. 1). $RO_2 + NO$ contributes $\sim 20\%$ – 50% to RO_2 loss, as NO and HO_2 concentrations are of the same order of magnitude in these cases.
- $RO_2 + NO$ dominates over $RO_2 + RO_2$ and $RO_2 + HO_2$ in almost all urban areas. Even in relatively clean urban areas such as Los Angeles during CalNex-LA in 2010 (point U in Fig. 1), average NO is ~ 1 ppb, still sufficiently high to ensure the dominance of $RO_2 + NO$ among the three pathways.
- Various chamber cases in the FIXCIT campaign (low to high OHR_{ext} ; low to high NO; points C_x in Fig. 1) are able to represent specific RO_2 fates that appear in different regions in the atmosphere.

On these plots, points for bad conditions (in terms of non-tropospheric photolysis) are not shown because of the lack of experimental interest. The triangle plots for OFR254-7 (including OFR254-7- iN_2O) in the same form (Supplement Fig. S1a, b) show no qualitative differences from the results of OFR254-70, implying that initial O_3 in OFR254 modes has only minor impacts on RO_2 fate. We see this result not only for well-known non-acyl RO_2 fate, but also for the aspects discussed in the following sections. The similarity between OFR254 modes can be explained by the minor effects of a lower O_3 on HO_x at relatively low OHR_{ext} (Peng et al., 2015). Cases at higher OHR_{ext} often have stronger non-tropospheric photolysis (Peng et al., 2016) and hence are more likely to be under bad conditions and are not shown in Figs. 1 and S1a, b. For simplicity, this similarity is not discussed further.

An important feature confirmed in Fig. 1 is that OFR- iN_2O modes effectively realize conditions of experimental interest with variable relative importance of $RO_2 + NO$ in RO_2 fate (Lambe et al., 2017; Peng et al., 2018). Tuning initially injected N_2O can achieve this goal (Fig. 2). While it is possible to reduce $RO_2 + HO_2$ in OFR185- iN_2O to negligible compared to $RO_2 + NO$ by increasing N_2O , this is not possible in OFR254-70- iN_2O due to fast NO oxidation by the large amounts of O_3 added in the reactor. Nevertheless, OFR254-70- iN_2O can still make $RO_2 + NO$ dominate over $RO_2 + HO_2$

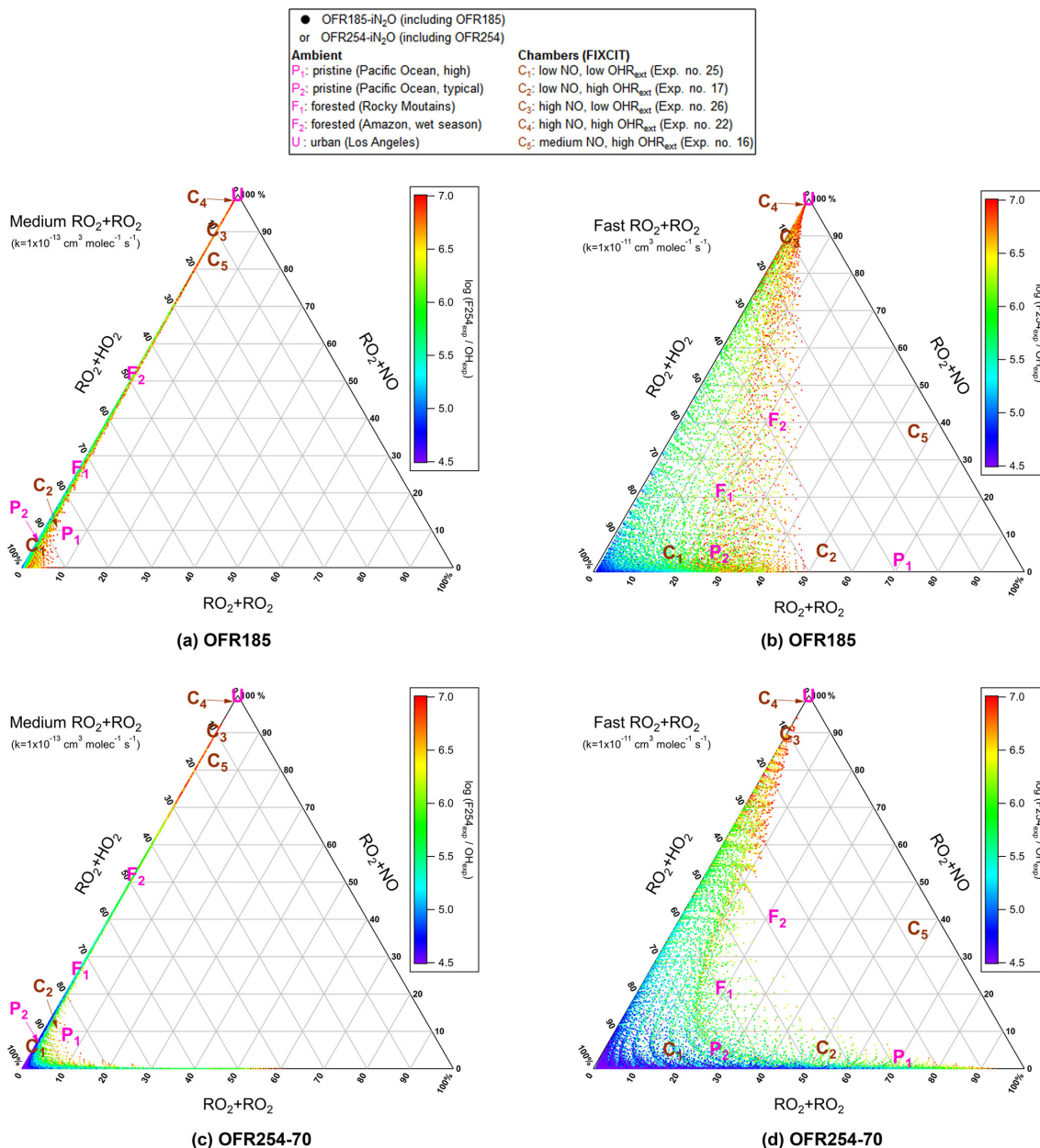


Figure 1. Triangle plots of RO₂ fate by RO₂ + HO₂, RO₂ + RO₂ and RO₂ + NO (without RO₂ + OH and RO₂ isomerization considered in the model) for RO₂ with the medium self- and cross-reaction rate constant ($1 \times 10^{-13} \text{ cm}^3 \text{ molecule}^{-1} \text{ s}^{-1}$) in (a) OFR185 (including OFR185-iN₂O) and (c) OFR254-70 (including OFR254-70-iN₂O) and for RO₂ with the fast self- and cross-reaction rate constant ($1 \times 10^{-11} \text{ cm}^3 \text{ molecule}^{-1} \text{ s}^{-1}$) in (b) OFR185 (including OFR185-iN₂O) and (d) OFR254-70 (including OFR254-70-iN₂O). Inclined tick values on an axis indicate the grid lines that should be followed (in parallel to the inclination) to read the corresponding values on this axis. The OFR data points are colored by the logarithm of the exposure ratio between 254 nm photon flux and OH, a measure of badness of OFR conditions in terms of 254 nm organic photolysis. Several typical ambient and chamber cases (see Table 2 for details on these cases) are also shown for comparison.

in RO₂ fate. OFR and chamber cases span a range of $\sim 0\%$ – $\sim 100\%$ in relative importance of RO₂ + NO in RO₂ fate (Fig. 2), suggesting that both chambers and OFRs are able to ensure the atmospheric relevance of RO₂ + NO in RO₂ fate.

Another important feature that can be easily seen in Fig. 1 is that medium-rate RO₂ + RO₂ (and hence also RO₂ + RO₂ slower than $10^{-13} \text{ cm}^3 \text{ molecule}^{-1} \text{ s}^{-1}$) is of negligible importance in the fate of RO₂ (Fig. 1a, c) in OFR185 (including OFR185-iN₂O), OFR254-70 (under most conditions, in-

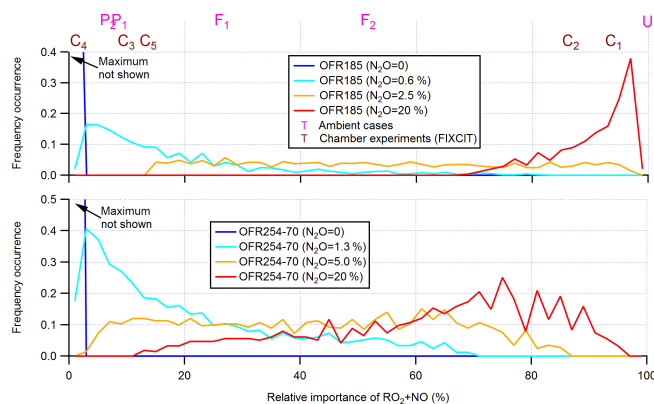


Figure 2. Frequency distributions of the relative importance of $\text{RO}_2 + \text{NO}$ in the fate of RO_2 (with medium self- and cross-reaction rate constant and without $\text{RO}_2 + \text{OH}$ and RO_2 isomerization considered) for OFR185 (including OFR185- iN_2O) and OFR254-70 (including OFR254-70- iN_2O). Distributions for several different N_2O levels are shown. Only good and risky conditions (in terms of non-tropospheric organic photolysis) are included in the distributions. Also shown is the relative importance of $\text{RO}_2 + \text{NO}$ for several typical ambient and chamber cases (see Table 2 for details on these cases).

cluding OFR254-70- iN_2O), chambers and the atmosphere. Thus, a very large subset of RO_2 types have only a minor or negligible contribution from $\text{RO}_2 + \text{RO}_2$ to their fate. This is already known for ambient RO_2 fate (Ziemann and Atkinson, 2012). The reason why this is also true in OFRs is that while OH is much higher than ambient levels, HO_2 and NO (high-NO conditions only) are also higher. One can easily verify that steady-state RO_2 concentrations (see Appendix B for details) would not deviate from ambient levels by orders of magnitude. The reactive fluxes of $\text{RO}_2 + \text{RO}_2$ in OFRs are thus not substantially different than in the atmosphere, while $\text{RO}_2 + \text{HO}_2$ and $\text{RO}_2 + \text{NO}$ (high-NO conditions only) are both faster in OFRs because of higher HO_2 and NO. The combined effect is a *reduced* relative importance of $\text{RO}_2 + \text{RO}_2$ in RO_2 fate in OFRs compared to the atmosphere. The only exception in OFRs occurs at very high VOC precursor concentrations (OHR_{ext} significantly $> 100 \text{ s}^{-1}$) in OFR254 (Fig. S2), in which OH levels are not substantially suppressed due to large amounts of O_3 (Peng et al., 2015). As a result, RO_2 concentration is remarkably increased by strong production, and $\text{RO}_2 + \text{RO}_2$ relative importance increases roughly quadratically and becomes significant.

The generally lower relative importance of $\text{RO}_2 + \text{RO}_2$ in OFRs than in the atmosphere is more obvious for the fate of RO_2 with fast $\text{RO}_2 + \text{RO}_2$ rate constants (Figs. 1b, d and 3). Although OFRs can reasonably reproduce RO_2 fates in typical low- and moderate- OHR_{ext} ambient environments (e.g., typical pristine and forested areas; Figs. 1b, d and 3) and low- OHR_{ext} chambers, OFR185 cannot achieve a relative importance of $\text{RO}_2 + \text{RO}_2$ significantly larger than 50 %, such as

Table 2. Several typical ambient and chamber (the FIXCIT campaign) cases that are compared to OFR cases.

Type	Label	Case	OHR _{VOC} (s^{-1})	OH	NO	HO ₂
Ambient	P ₁	Pristine (Pacific Ocean, high RO_2) ^a	1.9	0.39 ppt	1.9 ppt	11 ppt
	P ₂	Pristine (Pacific Ocean, typical) ^a	1	0.25 ppt	3 ppt	25 ppt
	F ₁	Forested (Rocky Mountains) ^b	N/A ^c	1 ppt	60 ppt	100 ppt
	F ₂	Forested (Amazon, wet season) ^d	9.6	1.2×10^6 molecules cm^{-3}	37 ppt	5.1×10^8 molecules cm^{-3}
	U	Urban (Los Angeles) ^e	25 ^f	1.5×10^6 molecules cm^{-3g}	1.5 ppb ^e	1.5×10^8 molecules cm^{-3g}
Chamber (FIXCIT)	C ₁	Exp. no. 25 ^h	30.5^i	3×10^6 molecules cm^{-3}	15 ppt	150 ppt
	C ₂	Exp. no. 17 ^h	116^i	1.2×10^6 molecules cm^{-3}	10 ppt	50 ppt
	C ₃	Exp. no. 26 ^h	32^i	2×10^7 molecules cm^{-3}	3.5 ppb	230 ppt
	C ₄	Exp. no. 22 ^h	147^i	2.3×10^6 molecules cm^{-3}	430 ppb	4.3 ppb
	C ₅	Exp. no. 16 ^h	45.7^i	4×10^6 molecules cm^{-3}	80 ppt	8 ppt

^a Wolfy et al. (2018) for the Atom-1 campaign; ^b Fry et al. (2013) for the BEACHON-ROMBAS campaign; ^c RO_2 concentration was given in Fry et al. (2013) (50 ppt) so that OHR_{VOC} is not needed for RO_2 fate estimation; ^d Daun Jeong and Saewung Kim, personal communication (2018), for the GoAmazon campaign (Martin et al., 2016, 2017); ^e Typical case in the CalNex-LA campaign (Ryerson et al., 2013); ^f Estimated (Peng et al., 2016); ^g Typical ambient value (Mao et al., 2009; Stone et al., 2012); ^h Data from Nguyen et al. (2014); ⁱ Initial value.

found in remote environments with higher VOC (e.g., P₁ in Fig. 1) and high-OHR_{ext} chamber experiments (e.g., C₂ and C₅ in Fig. 1; the distribution for C₂ is also shown in Fig. 3). In OFR254-70, a relative importance of RO₂ + RO₂ as high as ~ 90 % may be attained (Fig. S3). However, this requires very high OHR_{ext}, which leads to medium (and slower) RO₂ + RO₂ showing higher-than-ambient relative importance. In reality, fast RO₂ + RO₂ reactions all involve substituted RO₂, which almost certainly arises from and coexists with unsubstituted RO₂ (with slower self- and cross-reactions). Therefore, very high OHR_{ext} in OFR254 is not really suitable for attaining dominant RO₂ + RO₂ conditions. In OFR185, a higher OHR_{ext} generally also results in a higher RO₂ + RO₂ relative importance because of higher RO₂ production (Fig. S3). Nevertheless, higher OHR_{ext} is more likely to lead to risky or bad conditions (Fig. 3; Peng et al., 2016). It should be noted that although it is difficult to reliably achieve RO₂ + RO₂ with a relative importance larger than 50% in RO₂ fate in OFRs, the distributions of RO₂ + RO₂ relative importance in OFRs seem to be within a factor of 2 of those of field and aircraft campaigns (Fig. 3).

In the case of very fast RO₂ + RO₂, all features for fast RO₂ + RO₂ discussed above are still present (Fig. S1c, d). The only major difference between the results for fast RO₂ + RO₂ and very fast RO₂ + RO₂ is the significantly higher relative importance of RO₂ + RO₂ in RO₂ fate in the latter case, which is expected. In summary, fast RO₂ + RO₂ is not perfectly reproduced in OFRs in terms of relative importance in RO₂ fate, but it is significant when this pathway is also important in the atmosphere.

The HO_x recycling ratio β (see Sect. 2.3) is one of the key factors determining HO₂ in the OFR model, yet it is not well constrained. Although we make reasonable assumptions for it in the model input (see Sect. 2.3 for details), a sensitivity study to explore its effects is also performed here. For RO₂ with the fast self- and cross-reaction rate constant, we perform simulations with the HO_x recycling ratios fixed to a number of values from 0 (radical termination) to 2 (radical proliferation) in lieu of those calculated under the assumptions described in Sect. 2.3. As expected, the contribution of RO₂ + RO₂ to RO₂ fate increases monotonically between $\beta = 2$ and $\beta = 0$ (Fig. S4) as the recycling of the competing reactant HO₂ decreases. Nevertheless, the change in the average RO₂ + RO₂ relative importance from $\beta = 0$ to $\beta = 2$ is generally within a factor of 2. Thus, it still holds that the RO₂ + RO₂ relative importance in OFRs is generally lower than in the atmosphere. Only at $\beta \sim 0$ may OFR185 theoretically attain a relative importance of RO₂ + RO₂ of ~ 70 %, as in the P₁ case (pristine, but relatively high VOC; Fig. S5). Note that $\beta = 0$ for all VOC oxidation (including oxidation of intermediates) is extremely unlikely. In OFR254, even if RO₂ + RO₂ may contribute up to ~ 100 % to RO₂ fate at very high OHR_{ext} at $\beta = 0$, these conditions still also lead to significant RO₂ + RO₂ in the fate of RO₂ that self- and cross-reacts more slowly, which is not atmospherically relevant.

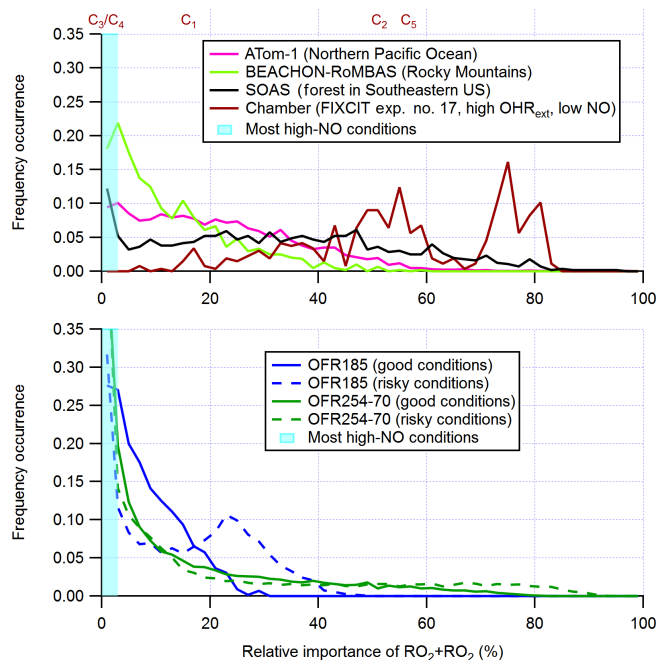


Figure 3. Frequency distributions of the relative importance of RO₂ + RO₂ in the fate of RO₂ (with fast self- and cross-reaction rate constant and without RO₂ + OH and RO₂ isomerization considered) for OFR185 (including OFR185-iN₂O), OFR254-70 (including OFR254-70-iN₂O), and a chamber experiment and in the atmosphere (a couple of different environments). The OFR distributions for good and risky conditions (in terms of 254 nm organic photolysis; see Table S1 for the definitions of these conditions) are shown separately. Also shown is the relative importance of RO₂ + RO₂ for several typical chamber cases (see Table 2 for details on these cases). The range of the RO₂ + RO₂ relative importance for most high-NO conditions is highlighted in cyan.

3.1.2 Acyl RO₂

As described in Sect. 2.1, the generic acyl RO₂ modeled in this study has the same loss pathways as RO₂ with the fast self- and cross-reaction rate constant, except for RO₂ + NO₂, which can be a significant acyl RO₂ loss pathway in OFRs as well as both chambers and the atmosphere. When this reaction is included in the simulations of acyl RO₂, it is a minor or negligible loss pathway of RO₂ at low N₂O, while it can be the dominant fate of acyl RO₂ at high N₂O (Fig. 4). In general, the RO₂ + NO₂ relative importance increases with initial N₂O. This is always true in OFR254-70-iN₂O between N₂O = 0.02 % and N₂O = 20 %, while in OFR185-iN₂O, the average relative contribution of RO₂ + NO₂ to RO₂ fate starts to decrease at N₂O ~ 10 % because RO₂ + NO regains some importance. This results from the HO_x suppression caused by high NO_y and strong NO production at high N₂O. Strong NO production increases its concentration and suppresses HO_x under these conditions, limiting the conversion of NO to NO₂. Because of the strong OH suppression by high NO_y,

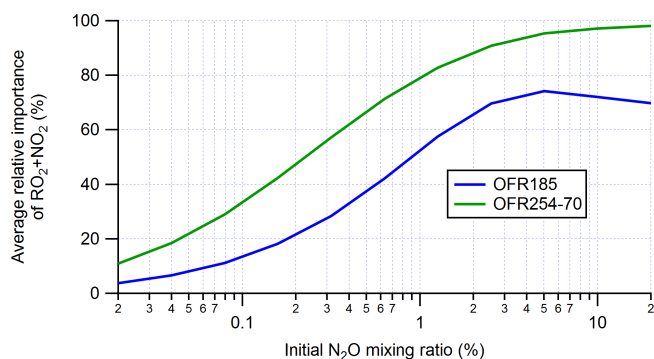


Figure 4. Average relative importance of $\text{RO}_2 + \text{NO}_2$ in acyl RO_2 fate ($\text{RO}_2 + \text{OH}$ and RO_2 isomerization not considered) in OFR185 (including OFR185- iN_2O) and OFR254-70 (including OFR254-70- iN_2O). The averages are calculated based on good and risky conditions (in terms of non-tropospheric organic photolysis) only.

at $\text{N}_2\text{O} \geq 10\%$, these conditions are not desirable (Peng et al., 2018).

The only difference between the simulations of acyl RO_2 and of the fast self- and cross-reacting non-acyl RO_2 is the quasi-irreversible reaction $\text{RO}_2 + \text{NO}_2 \rightarrow \text{RO}_2\text{NO}_2$ at room temperature, whose effects are revealed by a comparison of the triangle plots of the RO_2 fates in each case (Figs. 1b, d and S6). $\text{RO}_2 + \text{NO}_2$ is clearly dominant in acyl RO_2 fate in OFRs as long as $\text{RO}_2 + \text{NO}$ plays some role (not necessarily under high-NO conditions). In OFR185- iN_2O , the relative importance of $\text{RO}_2 + \text{RO}_2$ in the sum of the HO_2 , NO and RO_2 pathways is reduced (Fig. S6a) compared to that of non-acyl RO_2 with fast $\text{RO}_2 + \text{RO}_2$ (Fig. 1b) because $\text{RO}_2 + \text{NO}_2$ decreases acyl RO_2 concentration. Such a decrease is not significant in OFR254-70- iN_2O (Fig. S6b, compared to Fig. 1d), since for non-acyl RO_2 , it is already stored in the form of RO_2NO_2 as an RO_2 reservoir. In other words, the high initial O_3 greatly accelerates NO -to- NO_2 oxidation and shifts the equilibrium $\text{RO}_2 + \text{NO}_2 \leftrightarrow \text{RO}_2\text{NO}_2$ far to the right even for non-acyl RO_2 .

$\text{RO}_2 + \text{NO}_2$ is an inevitable and dominant sink of most acyl RO_2 in high- NO_x OFRs, though the extent of this dominance differs substantially among the different OFR operation modes. In OFR254-70- iN_2O , $\text{RO}_2 + \text{NO}$ makes a minor or negligible contribution to acyl RO_2 fate because the required high O_3 very rapidly oxidizes NO to NO_2 and leads to very low NO -to- NO_2 ratios (e.g., ~ 0.003 – 0.03 ; see Fig. S7). In OFR185- iN_2O , the contribution of $\text{RO}_2 + \text{NO}$ can be somewhat significant, with typical NO -to- NO_2 of ~ 0.03 – 0.4 . (Fig. S7). Urban NO -to- NO_2 ratios vary widely, for example (roughly, and excluding significant tails in the frequency distributions) 0.02–1 for Barcelona and 0.007–0.7 for Los Angeles and Pittsburgh (see Fig. S7). Given these variations among different urban areas, $\text{RO}_2 + \text{NO}$ and $\text{RO}_2 + \text{NO}_2$ for acyl RO_2 in OFR185- iN_2O can be regarded as relevant to urban atmospheres. Exceptions to the relevance of OFR185-

iN_2O occur during morning rush hours (e.g., see the high NO -to- NO_2 tail for the Pittsburgh case in Fig. S7), near major NO sources and/or in urban atmospheres with stronger NO emission intensity (e.g., Beijing, especially in winter; Fig. S7). In these cases, NO -to- NO_2 ratios may significantly exceed 1, and $\text{RO}_2 + \text{NO}$ may be the dominant acyl RO_2 loss pathway. Such high- NO conditions appear difficult to simulate in OFRs with the current range of techniques.

Acyl RO_2 is not the dominant type among RO_2 types under most conditions in OFRs, chambers and the atmosphere, since their formation usually requires multistep (at least 2 steps) oxidation via specific pathways leading to an oxidized end group (i.e., aldehyde and then acylperoxy). However, simulations using the GECKO-A model in urban (Mexico City) and forested (Rocky Mountains) atmospheres (Fig. S8) show that acyl RO_2 can still be a major (very roughly 1/3) component of RO_2 at ages of several hours or more. Therefore, acyl RO_2 chemistry in a high- NO OFR can significantly deviate from that in an urban atmosphere with NO_x dominating NO_x and can be relevant to an urban atmosphere with NO_2 dominating NO_x . On the other hand, a few theoretical studies suggested that H abstraction by the acylperoxy radical site from hydroperoxy groups close to the acylperoxy site in multifunctional acyl RO_2 may be extremely fast (Jørgensen et al., 2016; Knap and Jørgensen, 2017). If these theoretical predictions are sufficiently accurate, these acyl RO_2 types may exclusively undergo an intramolecular H shift to form non-acyl RO_2 or other radicals and prevent $\text{RO}_2 + \text{NO}_2$ from occurring even at very high (ppm level) NO_2 . However, this type of RO_2 is structurally specific and may not have strong impacts on the overall acyl RO_2 chemistry.

3.2 Simulations with all significant pathways

Since RO_2 isomerization does not significantly affect the generic RO_2 concentration, the two RO_2 fates that were recently found to be potentially important, i.e., $\text{RO}_2 + \text{OH}$ and RO_2 isomerization, can be discussed separately.

3.2.1 $\text{RO}_2 + \text{OH}$

In the troposphere, $\text{RO}_2 + \text{OH}$ is a minor (at low NO) or negligible (at high NO) RO_2 loss pathway (Fittschen et al., 2014; Assaf et al., 2016; Müller et al., 2016), as its rate constant is roughly an order of magnitude higher than that of $\text{RO}_2 + \text{HO}_2$ (Table 1), while the ambient OH concentration is on average 2 orders of magnitude lower than that of HO_2 (Mao et al., 2009; Stone et al., 2012; Fig. 5). We will not discuss $\text{RO}_2 + \text{OH}$ in the high- NO cases in detail. Simply put, the relative importance of $\text{RO}_2 + \text{OH}$ is generally negatively correlated with input N_2O in OFR- iN_2O , as NO_x suppresses OH and the relative importance of $\text{RO}_2 + \text{NO}$ increases. Below, we focus on low- NO (actually, for simplicity, zero- NO) conditions.

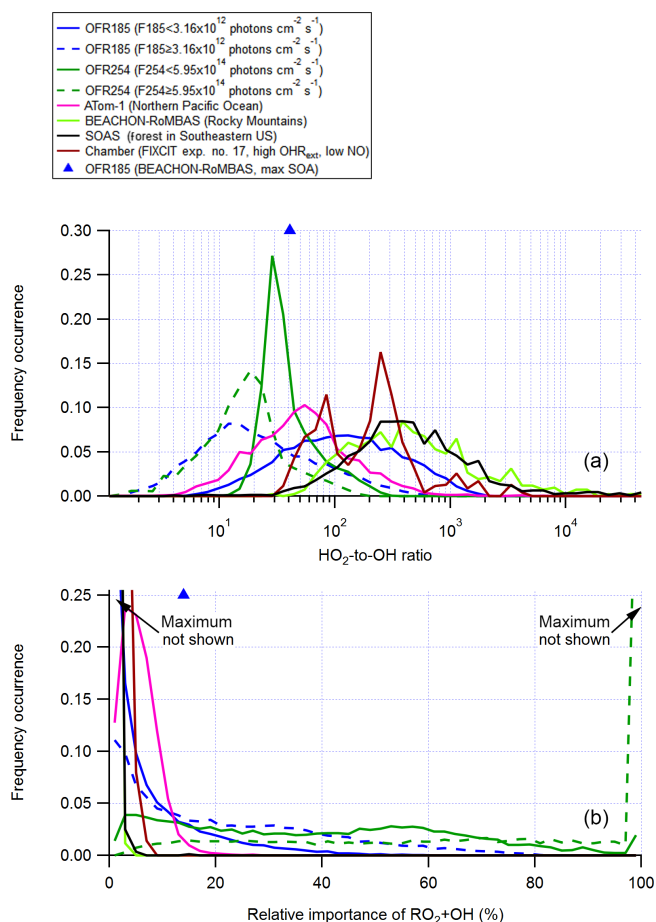


Figure 5. Frequency distributions of (a) the HO_2 -to-OH ratio and (b) the relative importance of $\text{RO}_2 + \text{OH}$ in the fate of RO_2 (with medium self- and cross-reaction rate constant) for OFR185 (including OFR185- iN_2O), OFR254-70 (including OFR254-70- iN_2O), and a chamber experiment and in the atmosphere (a couple of different environments). The OFR distributions for lower ($\text{F185} < 3.16 \times 10^{12} \text{ photons cm}^{-2} \text{ s}^{-1}$; $\text{F254} < 5.95 \times 10^{14} \text{ photons cm}^{-2} \text{ s}^{-1}$) and higher UV ($\text{F185} \geq 3.16 \times 10^{12} \text{ photons cm}^{-2} \text{ s}^{-1}$; $\text{F254} \geq 5.95 \times 10^{14} \text{ photons cm}^{-2} \text{ s}^{-1}$) are shown separately. Only good and risky conditions (in terms of non-tropospheric organic photolysis) are included in the distributions for OFRs. Also shown are the HO_2 -to-OH ratio and the relative importance of $\text{RO}_2 + \text{OH}$ for an OFR experiment with ambient air input in a field study (BEACHON-RoMBAS; Palm et al., 2016).

At $\text{N}_2\text{O} = 0$, it would be ideal if an HO_2 -to-OH ratio identical to the ambient values was realized in OFRs. In OFR185 cases with medium $\text{RO}_2 + \text{RO}_2$, an HO_2 -to-OH ratio around 100 occurs at a combination of low H_2O (of the order of 0.1%), low F185 (of the order of $10^{11} \text{ photons cm}^{-2} \text{ s}^{-1}$) and medium OHR_{ext} (10 – 100 s^{-1}) and also at medium F185 ($\sim 10^{12} \text{ photons cm}^{-2} \text{ s}^{-1}$) combined with very high OHR_{ext} ($\sim 1000 \text{ s}^{-1}$, Fig. S9). Under both sets of conditions, relatively high external OH reactants suppress OH, whose production is relatively weak, and convert some OH into HO_2

through HO_x recycling in organic oxidation (e.g., via alkoxy radical chemistry). The reason why such an OH-to- HO_2 conversion is needed to attain an ambient-like HO_2 -to-OH ratio is that OFR185 is unable to achieve this via the internal (mainly assisted by O_3) interconversion of HO_x . This inability is most evident when F185 (10^{13} – $10^{14} \text{ photons cm}^{-2} \text{ s}^{-1}$) and H_2O (of the order of 1 %) are high and OHR_{ext} is low ($< \sim 10 \text{ s}^{-1}$; Fig. S9). Under these conditions, OH production by H_2O photolysis is so strong that the HO_2 -to-OH ratio is lowered to ~ 1 , since OH and H (which recombines with O_2 to form HO_2) are produced in equal amounts from H_2O photolysis. As the $\text{RO}_2 + \text{OH}$ rate constant is only roughly 1 order of magnitude higher than that for $\text{RO}_2 + \text{HO}_2$, slightly lower HO_2 -to-OH ratios (e.g., ~ 30) suffice to keep $\text{RO}_2 + \text{OH}$ minor in this case. A combination of UV and H_2O that are not very high and a moderate OHR_{ext} that is able to convert some OH to HO_2 and somewhat elevate the HO_2 -to-OH ratio results in minor relative importance for $\text{RO}_2 + \text{OH}$ (Figs. S9 and S10).

In OFR254-70, it is more difficult to reach an HO_2 -to-OH ratio of ~ 100 , which can only be realized at a combination of very low H_2O and F254 ($\sim 0.07\%$ and $\sim 5 \times 10^{13} \text{ photons cm}^{-2} \text{ s}^{-1}$, respectively) and very high OHR_{ext} ($\sim 1000 \text{ s}^{-1}$). This is mainly due to high O_3 in OFR254-70, which controls the HO_x interconversion through $\text{HO}_2 + \text{O}_3 \rightarrow \text{OH} + 2\text{O}_2$ and $\text{OH} + \text{O}_3 \rightarrow \text{HO}_2 + \text{O}_2$ and makes both OH and HO_2 more resilient to changes due to OHR_{ext} (Peng et al., 2015). Even without H_2O photolysis at 185 nm as a major HO_2 source, the HO_x interconversion controlled by O_3 in OFR254-70 still brings the HO_2 -to-OH ratio to ~ 1 in the case of minimal external perturbation (see the region at the highest H_2O and UV and $\text{OHR}_{\text{ext}} = 0$ in the OFR254-70 part of Fig. S9). This ratio cannot be easily elevated in OFR254-70 because of the resilience of OH to suppression for this mode (Peng et al., 2015). Thus, this ratio is relatively low (< 30) under most conditions (Fig. S9), and consequently (and undesirably) $\text{RO}_2 + \text{OH}$ is a major RO_2 fate in OFR254-70. There is an exception at relatively low H_2O and UV with very high OHR_{ext} (Fig. S10); however, these conditions are undesirable in terms of non-tropospheric organic photolysis (Peng et al., 2016).

Only the results of RO_2 with medium $\text{RO}_2 + \text{RO}_2$ are discussed in this section. Those of RO_2 with the fast $\text{RO}_2 + \text{RO}_2$ are not shown as they are not qualitatively different. In OFR185, for the fast self- and cross-reacting RO_2 , $\text{RO}_2 + \text{RO}_2$ is relatively important at high OHR_{ext} ($> \sim 100 \text{ s}^{-1}$; Fig. S3), while $\text{RO}_2 + \text{OH}$ is a major RO_2 fate at low OHR_{ext} (generally of the order of 10 s^{-1} or lower) and relatively high H_2O and UV (Fig. S10). These two ranges of conditions are relatively far away from each other, and hence there is no condition under which $\text{RO}_2 + \text{RO}_2$ and $\text{RO}_2 + \text{OH}$ are both major pathways that compete, which simplifies understanding RO_2 fate. However, in OFR254-70, some conditions may lead to both significant $\text{RO}_2 + \text{RO}_2$ (for the fast self- and cross-reacting RO_2) and $\text{RO}_2 + \text{OH}$ (e.g., $\text{H}_2\text{O} \sim 0.5\%$,

$F_{254} \sim 1 \times 10^{15}$ photons $\text{cm}^{-2} \text{s}^{-1}$ and $\text{OHR}_{\text{ext}} \sim 100 \text{s}^{-1}$). Nevertheless, as long as $\text{RO}_2 + \text{OH}$ plays a major role, these conditions do not bear much experimental interest and thus do not need to be discussed in detail.

3.2.2 RO_2 isomerization

RO_2 isomerization is a first-order reaction. For this type of reaction to occur, RO_2 does not need any other species but only a sufficiently long lifetime against all other reactants combined, as most RO_2 isomerization rate constants are $< 10 \text{s}^{-1}$. Radical (OH , HO_2 , NO , etc.) concentrations in OFRs are much higher than ambient levels and may shorten RO_2 lifetimes compared to those in the troposphere. Possibly reduced RO_2 lifetimes naturally raise concerns over the potentially diminished importance of RO_2 isomerization in OFRs.

In this section we examine generic RO_2 lifetimes against all reactions (calculated without RO_2 isomerization taken into account) in OFR (including OFR- iN_2O) cases (for the medium $\text{RO}_2 + \text{RO}_2$ case) and compare them with the RO_2 lifetimes in recent major field and aircraft campaigns in relatively clean environments and a field campaign in an urban area (CalNex-LA), as well as a low-NO chamber experiment (Fig. 6). Indeed, RO_2 lifetimes in clean ambient cases and in chambers with near-ambient radical levels are generally much longer than those in OFRs. The RO_2 lifetime distribution of the explored good and risky cases in OFR254-70 (including OFR254-70- iN_2O) barely overlaps the ambient and chamber cases, while in OFR185 (including OFR185- iN_2O), the RO_2 lifetime can be as long as $\sim 10 \text{s}$, which is longer than in urban areas and roughly at the lower end of the range of ambient RO_2 lifetimes in clean environments (Fig. 6). The longest RO_2 lifetime in OFR185 occurs at very low F_{185} (of the order of 10^{11} photons $\text{cm}^{-2} \text{s}^{-1}$) and H_2O ($\sim 0.1 \%$; Fig. S11) when HO_x is low. In OFR254-70, for RO_2 to survive for $\sim 10 \text{s}$, in addition to very low UV and H_2O , high OHR_{ext} is also needed (Fig. S11). High- OHR_{ext} conditions in OFR254-70 cause OH suppression and a decrease in HO_x concentration and hence result in relatively long RO_2 lifetimes. However, the strong OH suppression is likely to create bad conditions (high contribution of non-tropospheric photolysis) (Peng et al., 2016). Low- OHR_{ext} conditions do not lead to long RO_2 lifetimes in OFR254-70 even at very low F_{254} and H_2O , since O_3 -assisted HO_x recycling prevents a very low HO_x level even if HO_x primary production is low (Peng et al., 2015)

An RO_2 lifetime (without RO_2 isomerization included) of 10s leads to a relative importance of isomerization of 50% in the total fate (including all loss pathways) of RO_2 with an isomerization rate constant of 0.1s^{-1} , which is a typical order of magnitude for isomerization rate constants of multifunctional RO_2 with hydroxyl and hydroperoxy substituents (Fig. 6; Crouse et al., 2013; D'Ambro et al., 2017; Praske et al., 2018). Although a 50% relative importance of isomeriza-

tion under some OFR conditions is still lower than those in relatively low-NO ambient environments and low-NO chambers, this relative importance should certainly be deemed major and far from negligible as some have speculated (Crouse et al., 2013). Other monofunctional RO_2 (with peroxy radical site only) and bifunctional RO_2 with a peroxy radical site and a carbonyl group isomerize so slowly ($\sim 0.001\text{--}0.01 \text{s}^{-1}$) that their isomerizations are minor or negligible loss pathways in the atmosphere, chambers and OFRs with RO_2 lifetimes around 10s (Fig. 6). Isomerizations of other types of multifunctional RO_2 (e.g., multifunctional acyl RO_2 with hydroxyl and hydroperoxy substituents at favorable positions) are extremely fast (rate constants up to 10^6s^{-1} ; Jørgensen et al., 2016; Knap and Jørgensen, 2017) and always dominate in their fates in the relatively low-NO atmosphere as well as in chambers and OFRs with RO_2 lifetimes around 10s .

In the discussion about RO_2 isomerization above (as in the $\text{RO}_2 + \text{OH}$ exploration in Sect. 3.2.1), we only examine low-NO (or zero-NO for simplicity) conditions with medium $\text{RO}_2 + \text{RO}_2$. In high-NO environments, e.g., polluted urban atmospheres with NO of at least ~ 10 ppb and high-NO OFRs in the iN_2O modes, the RO_2 lifetime is so short that isomerization is no longer a major fate for any but the most rapidly isomerizing multifunctional RO_2 types discussed above. NO measured in Los Angeles during the CalNex-LA campaign (Ortega et al., 2016) was only ~ 1 ppb, which would allow RO_2 to survive for a few seconds and isomerize (Fig. 6), even in an urban area.

The OFR simulations for the discussions about RO_2 isomerization are the same as those conducted to study $\text{RO}_2 + \text{OH}$, i.e., the ones with medium $\text{RO}_2 + \text{RO}_2$ and $\text{RO}_2 + \text{OH}$ included. For fast RO_2 self- and cross-reaction cases, RO_2 lifetimes may be significantly shorter than for RO_2 with the medium self- and cross-reaction rate constant at high OHR_{ext} ($> \sim 100 \text{s}^{-1}$) in OFR185 (Fig. S3). These high- OHR_{ext} conditions are likely to be risky or bad (of little experimental interest) (Peng et al., 2016) and thus do not need to be discussed further in detail. OFR254-70 (a zero-NO mode) does not generate good or risky (of at least some experimental interest in terms of non-tropospheric organic photolysis) conditions, also leading to low-NO-atmosphere-relevant RO_2 lifetimes (Fig. 6). RO_2 types with faster self- and cross-reaction rate constants have even shorter lifetimes in OFR254-70 and will not be discussed further.

3.3 Guidelines for OFR operation

In this section we discuss OFR operation guidelines for atmospherically relevant RO_2 chemistry, with a focus on OFR185 and OFR254 (zero-NO modes). Since $\text{RO}_2 + \text{HO}_2$ and $\text{RO}_2 + \text{NO}$ both can vary from negligible to dominant RO_2 fate in OFRs, chambers and the atmosphere (Figs. 1 and 2), these two pathways are not a concern in OFR atmospheric relevance considerations, and neither is $\text{RO}_2 + \text{RO}_2$. Medium or slower $\text{RO}_2 + \text{RO}_2$ is minor or negligible in the atmosphere

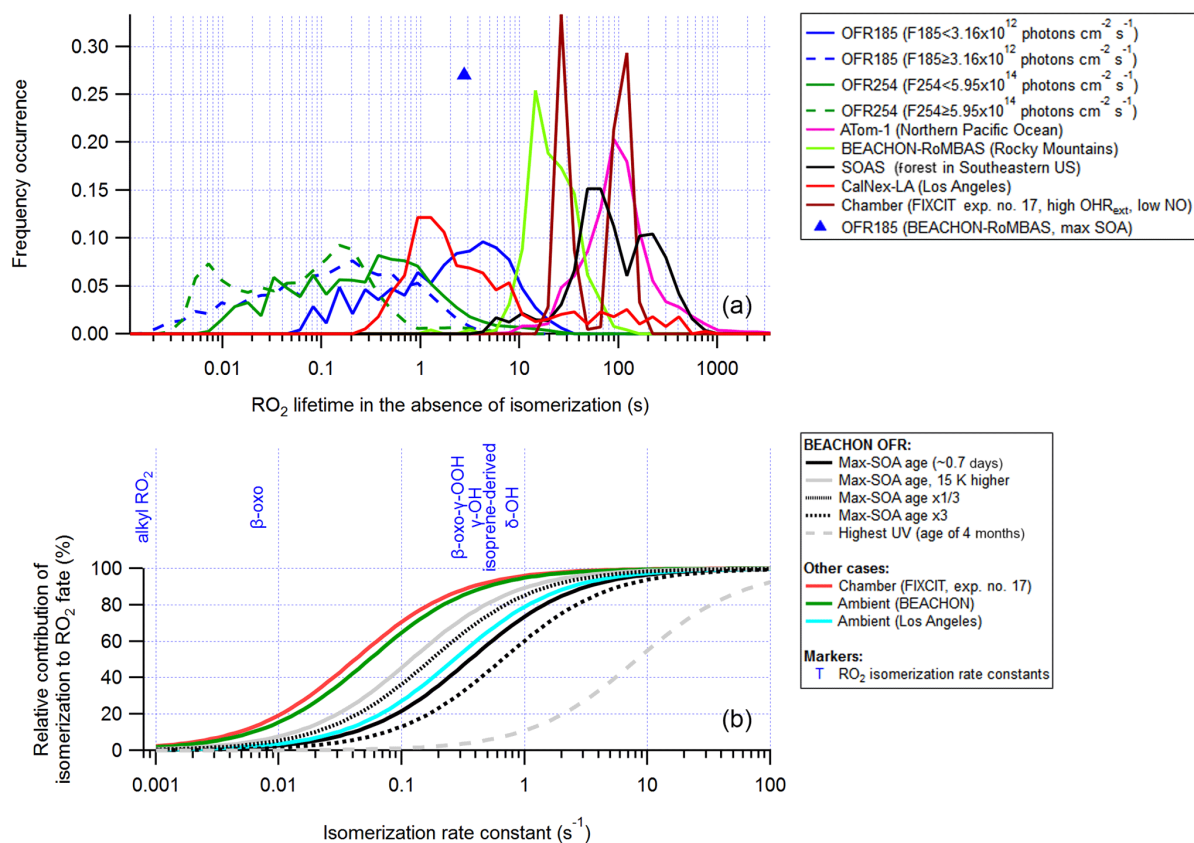


Figure 6. (a) Same format as Fig. 5, but for RO_2 lifetime (RO_2 isomerization included in the model but excluded from lifetime calculation). (b) Relative contribution of isomerization to RO_2 fate as a function of RO_2 isomerization rate constant in several model cases for OFR experiments in the BEACHON-RoMBAS campaign (Palm et al., 2016), in a chamber experiment and in two ambient cases. Isomerization rate constants of several RO_2 types (Crounse et al., 2013; Praske et al., 2018) are also shown.

and chambers, as well as in OFRs, as long as high OHR_{ext} is avoided in OFR254 (Fig. S2). Fast $RO_2 + RO_2$ is somewhat less important in OFRs than in the atmosphere (Figs. 1b, d and 3), but is still qualitatively atmospherically relevant, given the uncertainties associated with the HO_x recycling ratios of various reactive systems and the huge variety of RO_2 types (and hence $RO_2 + RO_2$ rate constants).

Accordingly, we focus on the atmospheric relevance of $RO_2 + OH$ and RO_2 isomerization, i.e., their relative contributions close to ambient values. Under typical high-NO conditions, $RO_2 + NO$ dominates RO_2 fate and $RO_2 + OH$ is negligible. High NO also shortens the RO_2 lifetime enough to effectively inhibit RO_2 isomerization. Both the dominance of $RO_2 + NO$ and the inhibition of RO_2 isomerization also occur in the atmosphere and in chambers, so high-NO OFR operation (typically $NO > 10$ ppb) represents these pathways realistically. Some care is, however, required with the $RO_2 + OH$ and RO_2 isomerization pathways at low NO. Since $RO_2 + HO_2$ in OFRs is always a major RO_2 fate at low NO and $RO_2 + RO_2$ is generally not problematic, $RO_2 + OH$ and $RO_2 + HO_2$ can be kept atmospherically relevant as long

as the HO_2 -to- OH ratio is close to 100 (the ambient average). In addition, the RO_2 lifetime (calculated without RO_2 isomerization taken into account) should be at least around 10 s.

Practically, OH production should be limited to achieve this goal. Too-strong OH production at high H_2O and UV can elevate OH and HO_2 concentrations, which shortens RO_2 lifetime and decreases the HO_2 -to- OH ratio to ~ 1 (see Sect. 3.2.1). OH production is roughly proportional to both H_2O and UV (Peng et al., 2015), so it can be limited by reducing either or both. However, H_2O and UV have different effects on non-tropospheric organic photolysis. At a certain OHR_{ext} , the OH production rate roughly determines the OH concentration in OFRs. Reducing UV decreases both OH and UV roughly proportionally (Peng et al., 2015), and hence changes in $F185_{exp} / OH_{exp}$ and $F254_{exp} / OH_{exp}$ are small (Peng et al., 2016); i.e., non-tropospheric organic photolysis does not become significantly worse if UV is reduced. By contrast, if H_2O is reduced without also decreasing UV, $F185_{exp} / OH_{exp}$ and $F254_{exp} / OH_{exp}$ both increase, signifying a stronger relative importance of non-tropospheric pho-

tolysis. Therefore, reducing UV is strongly preferred as an OH production limitation method and is effective in making both $\text{RO}_2 + \text{OH}$ and RO_2 isomerization more atmospherically relevant.

To further explore the effects of UV reduction on the $\text{RO}_2 + \text{OH}$ (Fig. 5) and RO_2 isomerization (Fig. 6) pathways, we divide our OFR case distributions into higher UV and lower UV classes, with the boundary being the midlevel (in logarithmic scale) UV in the explored range. The distributions for lower UV conditions (solid lines in Figs. 5 and 6) are clearly closer to the ambient cases (i.e., HO_2 -to-OH ratio closer to 100, smaller $\text{RO}_2 + \text{OH}$ relative importance and longer RO_2 lifetime).

Since OFR254 is unable to achieve both conditions with at least some experimental interest (i.e., with sufficiently low non-tropospheric photolysis) and an atmospherically relevant RO_2 lifetime, we now discuss preferable conditions for OFR185 only. As F185 close to or lower than 10^{12} photons $\text{cm}^{-2} \text{s}^{-1}$ is needed for the RO_2 lifetime to be around 10 s or longer (Fig. S11), the OH concentration under preferable conditions for atmospherically relevant RO_2 chemistry ($\sim 10^9$ molecules cm^{-3} or lower) is much lower than the maximum that OFR185 can physically reach ($\sim 10^{10}$ – 10^{11} molecules cm^{-3}). Furthermore, lower OH production leads to higher susceptibility to OH suppression by external OH reactants (Peng et al., 2015), which can create non-tropospheric photolysis problems (Peng et al., 2016). We thus recommend H_2O as high as possible to maintain practically high OH while allowing lower UV to limit the importance of non-tropospheric organic photolysis.

The performance of various OFR185 conditions at high H_2O (2.3 %) is illustrated in Fig. 7 as a function of F185 and OHR_{ext} . The three criteria for the performance, i.e., RO_2 lifetime (calculated without RO_2 isomerization considered), relative importance of $\text{RO}_2 + \text{OH}$ and $\log(\text{F254}_{\text{exp}} / \text{OH}_{\text{exp}})$ (a measure of 254 nm non-tropospheric photolysis, which is usually worse than that at 185 nm; Peng et al., 2016), are shown. At F185 of $\sim 10^{11}$ – 10^{12} photons $\text{cm}^{-2} \text{s}^{-1}$ and OHR_{ext} around or lower than 10 s^{-1} , all three criteria are satisfied. Since UV (and hence OH production) is relatively low, a low OHR_{ext} ($\sim 10 \text{ s}^{-1}$) is required to avoid heavy OH suppression and keep conditions good (green area in Fig. 7c). Nevertheless, risky conditions ($\log(\text{F254}_{\text{exp}} / \text{OH}_{\text{exp}}) < 7$; light red area in Fig. 7c) may also bear some experimental conditions depending on the type of VOC precursors (specifically on their reactivity toward OH, their photolability at 185 and 254 nm, and the same quantities for their oxidation intermediates; Peng et al., 2016; Peng and Jimenez, 2017). Thus, higher OHR_{ext} (up to $\sim 100 \text{ s}^{-1}$) may also be considered in OFR experiments with some precursors (e.g., alkanes). In practice, the preferred conditions may require F185 even lower than that our lowest simulated lamp setting (Li et al., 2015). Such a low F185 may be realized, e.g., by partially blocking 185 nm photons using nontransparent lamp sleeves

with evenly placed holes that allow for some 185 nm transmission.

Under these preferred conditions, OH concentration in OFR185 is $\sim 10^9$ molecules cm^{-3} , equivalent to a photochemical age of ~ 1 eq. days for a typical residence time of 180 s. This is much shorter than ages corresponding to the maximal oxidation capacity of OFRs (usually eq. weeks or months; Peng et al., 2015), but it is similar to the ages of the maximal organic aerosol formation in OFRs processing ambient air (Tkacik et al., 2014; Ortega et al., 2016; Palm et al., 2016). We show the maximal SOA formation case in the OFR185 experiments in the BEACHON-RoMBAS campaign in the Rocky Mountains (Palm et al., 2016) as an example (Figs. 5 and 6). During the campaign, relative humidity was high ($> 60\%$ in most of the period), OHR_{ext} was estimated to be relatively low ($\sim 15 \text{ s}^{-1}$) in this forested area and UV in the OFR was limited in the case of the maximal SOA formation age (~ 0.7 eq. days). All these physical conditions were favorable for atmospherically relevant RO_2 fate (Figs. 5 and 6). $\text{RO}_2 + \text{OH}$ was minor in this case and the relative importance of RO_2 isomerization in RO_2 fate in the OFR was within a factor of ~ 2 of that in the atmosphere for all RO_2 (regardless of the isomerization rate constant) during the BEACHON-RoMBAS campaign (Fig. 6). The effect of UV on the relative importance of RO_2 isomerization for this example is also illustrated in Fig. 6. In the sensitivity case with a lower age, lower UV results in a larger contribution of isomerization to RO_2 fate, while the relative importance of RO_2 isomerization is lower in a sensitivity case with an age 3 times that of the maximal SOA formation. In an extreme sensitivity case with the highest UV in the range of this study (with an age of 4 eq. months), RO_2 isomerization becomes minor or negligible for all RO_2 except extremely rapidly isomerizing ones.

The discussions above indicate that the atmospheric relevance of gas-phase RO_2 chemistry in OFRs deteriorates as the photochemical age over the whole residence time (180 s) increases. To reach longer ages, longer residence times (with UV still being low) can be adopted. However, OFR residence times > 10 min tend to be limited by the increasing importance of wall losses (Palm et al., 2016). As a result, longer residence times can only increase photochemical age in OFRs up to about a week. This implies that in OFR cases with ages much higher than that of maximal SOA formation (corresponding to the heterogeneous oxidation stage of SOA), the atmospheric relevance of gas-phase RO_2 chemistry in the SOA formation stage (before the age of maximal SOA formation) often cannot be ensured. However, under those conditions new SOA formation is typically not observed, and the dominant process affecting OA is heterogeneous oxidation of the preexisting OA (Palm et al., 2016). If the heterogeneous oxidation of newly formed SOA is of interest, a two-stage solution may be required. Lower UV can be used in the SOA formation stage to keep the atmospheric relevance of the gas-phase chemistry, while high UV

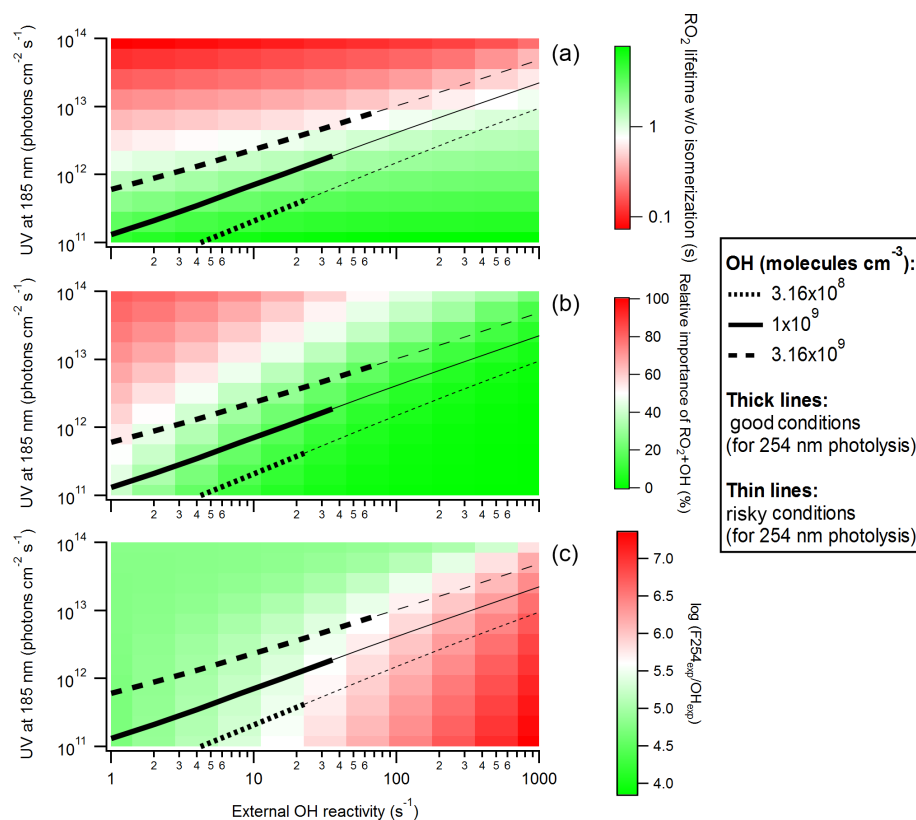


Figure 7. (a) RO_2 lifetime in the absence of isomerization, (b) relative importance of $\text{RO}_2 + \text{OH}$ in RO_2 fate, and (c) logarithm of the exposure ratio between 254 nm photon flux and OH as a function of 185 nm photon flux and external OH reactivity for OFR185 at $\text{N}_2\text{O} = 0$ and $\text{H}_2\text{O} = 2.3\%$. Three lines denoting conditions leading to OH of 3.16×10^8 , 1×10^9 and 3.16×10^9 molecules cm^{-3} are added in each panel. The thick and thin parts of these lines correspond to good and risky conditions (in terms of 254 nm organic photolysis, which is usually worse than 185 nm organic photolysis; Peng et al., 2016), respectively.

can be used in the heterogeneous aging stage to reach a high equivalent age. The latter approach is viable since heterogeneous oxidation of SOA by OH is slow and particle-phase chemistry is not strongly affected by gas-phase species except OH when OH is very high (Richards-Henderson et al., 2015, 2016; Hu et al., 2016). This two-stage solution may be realized through a cascade-OFr system or UV sources at different intensities within an OFr (e.g., spliced lamps).

Praske et al. (2018) measured RO_2 isomerization rate constants at 296 and 318 K and observed an increase in the rate constants by a factor of ~ 5 on average. A 15 K temperature increase in OFrs would lead to RO_2 isomerization being accelerated by a factor of ~ 3 , while other major gas-phase radical reactions have weak or no temperature dependence (e.g., $\sim 7\%$, $\sim 5\%$, $\sim 6\%$ and $\sim 19\%$ slowdowns for isoprene+OH, toluene + OH, typical $\text{RO}_2 + \text{NO}$ and $\text{RO}_2 + \text{HO}_2$, respectively; Atkinson and Arey, 2003; Ziemann and Atkinson, 2012). As a consequence, the relative importance of RO_2 isomerization in RO_2 fate in OFrs can be elevated and closer to atmospheric values (Fig. 6). Nevertheless, a 15 K increase in temperature may also result in some OA evaporation (Huffman et al., 2009; Nault et al.,

2018). Besides, the reduction of acylperoxy nitrate formation in OFrs, which may be useful to mimic some urban environments where NO plays a larger role in acyl RO_2 fate (see Sect. 3.1.2), is unlikely to be achieved by increasing OFr temperature. The O–N bond energy of acylperoxy nitrates is $\sim 28 \text{ kcal mol}^{-1}$ (Orlando and Tyndall, 2012), which can be taken as an approximate reaction energy of their decomposition. Then a 20 K temperature increase results in the equilibrium constant of $\text{acyl RO}_2 + \text{NO}_2 \leftrightarrow \text{acyl RO}_2\text{NO}_2$ being shifted toward $\text{RO}_2 + \text{NO}_2$ by a factor of ~ 20 . However, this shift is still too small relative to the equilibrium constant itself. It can be deduced by a simple calculation that for the generic acyl RO_2 in this study in an OFr at 318 K (20 K higher than room temperature) with NO_2 of 10^{12} molecules cm^{-3} (a relatively low level in typical OFr- iN_2O experiments; Peng et al., 2018), $\sim 0.1\%$ of the total amount of acyl $\text{RO}_2 + \text{acyl RO}_2\text{NO}_2$ will be present in the form of acyl RO_2 . Even if acylperoxy nitrate decomposition is 20 times faster than at room temperature and the formed acyl RO_2 can irreversibly react with NO and decrease the acylperoxy nitrate concentration, this effect is small: typically up to an approximate 20 % decrease in acylperoxy ni-

trate and usually negligible changes in NO and NO₂. The minor effect is due to (i) an acylperoxy concentration that is still very low, (ii) an NO concentration that is much lower than NO₂ and (iii) an acylperoxy nitrate decomposition lifetime that is still of the order of minutes.

As discussed above, high H₂O, low UV and low OHR_{ext} are recommended for keeping the atmospheric relevance of RO₂ chemistry in OFRs. These three requirements are also part of the requirements for attaining good high-NO conditions in OFR185-iNO (the OFR185 mode with initial NO injection; Peng and Jimenez, 2017). In addition to these three, an initial NO of several tens of ppb is also needed to obtain a good high-NO condition in OFR185-iNO. Under these conditions, RO₂ + NO dominates over RO₂ + HO₂ and hence RO₂ + OH; UV is low, the photochemical age is typically ~ 1 eq. days and the RO₂ lifetime can be a few seconds. Therefore, these conditions are a good fit for studying the environments in relatively clean urban areas, such as Los Angeles during CalNex-LA (Ortega et al., 2016), where NO is high enough that the dominant bimolecular fate of RO₂ is RO₂ + NO but low enough to maintain RO₂ lifetimes that allow for the most common RO₂ isomerizations.

As RO₂ fate in OFRs is a highly complex problem and it can be tricky to find suitable physical conditions to simultaneously achieve experimental goals and keep the atmospheric relevance of the chemistry in OFRs, we provide here an OFR RO₂ Fate Estimator (in the Supplement) to qualitatively aid experimental planning. The OFR RO₂ Fate Estimator couples the OFR Exposure Estimator (Peng et al., 2016, 2018) to a general RO₂ fate estimator (also in the Supplement; see Fig. S12 for a screenshot of its layout). The OFR Exposure Estimator updated in this study also contains estimation equations for the HO₂-to-OH ratio in OFR185 (in OFR254, RO₂ fate is always atmospherically irrelevant at low NO, while at high NO, RO₂ + NO dominates and a detailed RO₂ fate analysis is no longer needed). In the general RO₂ fate estimator, all RO₂ reactant concentrations and all RO₂ loss pathway rate constants can be specified. Thus, the general RO₂ fate estimator can also be applied to the atmosphere and chamber experiments, in addition to OFRs. When applied to OFRs, the general RO₂ fate estimator is provided by the OFR RO₂ Fate Estimator with quantities estimated in the OFR Exposure Estimator (e.g., OH and NO). RO₂ concentration and fate are calculated according to Appendix B in the RO₂ fate estimators.

4 Conclusions

We investigated RO₂ chemistry in OFRs with an emphasis on its atmospheric relevance. All potentially major loss pathways of RO₂, i.e., reactions of RO₂ with HO₂, NO and OH, of acyl RO₂ with NO₂, and self- and cross-reactions of RO₂ and RO₂ isomerization, were studied and their relative importances in RO₂ fate were compared to those in the at-

mosphere and chamber experiments. OFRs were shown to be able to tune the relative importance of RO₂ + HO₂ vs. RO₂ + NO by injecting different amounts of N₂O. For many RO₂ types (including all unsubstituted non-acyl RO₂ and substituted secondary and tertiary RO₂), their self-reactions and the cross-reaction between them are minor or negligible in the atmosphere and chambers. This is also the case in OFR185 (including OFR185-iN₂O) and OFR254-iN₂O; however, those RO₂ self- and cross-reactions can be important at high precursor concentrations (OHR_{ext} > 100 s⁻¹) in OFR254. For substituted primary RO₂ and acyl RO₂, their self- and cross-reactions (including the ones with RO₂ whose self-reaction rate constants are slower) can play an important role in RO₂ fate in the atmosphere and chambers and may also be major RO₂ loss pathways in OFRs, although they are somewhat less important in OFRs than in the atmosphere. Acylperoxy nitrates are the dominant sink of acyl RO₂ at high NO_x in OFRs (particularly in OFR254-iN₂O for which RO₂ + NO is negligible for acylperoxy loss), while there is only a minor reservoir of acyl RO₂ in the atmosphere under most conditions except in urban atmospheres, where RO₂ + NO and RO₂ + NO₂ can both be the dominant acylperoxy loss pathway depending on conditions. In chambers, most acyl RO₂ can be stored in the form of acylperoxy nitrates if NO₂ is very high (hundreds of ppb to ppm level).

Besides the abovementioned well-known pathways, RO₂ + OH and RO₂ isomerization may also play an important role in RO₂ fate and sometimes results in atmospherically irrelevant RO₂ chemistry in OFRs. Here we summarize the main findings about all the pathways and the related guidelines for OFR operation.

- Under typical high-NO conditions, RO₂ + NO dominates RO₂ fate and the RO₂ lifetime is too short to allow for most RO₂ isomerizations, regardless of whether in the atmosphere, chambers or OFRs, thus raising no concern about the atmospheric relevance of the OFR RO₂ chemistry.
- Under low-NO conditions, OFR254 cannot yield any physical conditions leading to a sufficiently long RO₂ lifetime for its isomerization because of the high radical levels and their resilience to external perturbations in OFR254.
- In OFR185 with strong OH production (and hence high OH), RO₂ + OH and RO₂ isomerization may strongly deviate from that in the atmosphere (becoming important and negligible, respectively, for relatively rapidly isomerizing RO₂; rate constants of the order of 0.1 s⁻¹).
- To attain both atmospherically relevant VOC and RO₂ chemistries, OFR185 requires high H₂O, low UV and low OHR_{ext}. These conditions ensure minor or negligible RO₂ + OH and a relative importance of RO₂ isomerization in RO₂ fate in OFRs within a factor of ~ 2 of that in the atmosphere.

- Under conditions allowing both VOC and RO₂ chemistries to be atmospherically relevant, the maximal photochemical age that can be reached is limited to a few eq. days. This age roughly covers the period required for maximum SOA formation in ambient air.
- To most realistically study much higher ages for SOA functionalization and fragmentation by heterogeneous oxidation, a sequence of low-UV SOA formation followed by a high UV condition (in the same reactor or in cascade reactors) may be needed.
- High H₂O, low UV and low OHR_{ext} in the OFR185-iNO mode can achieve conditions relevant to clean urban atmosphere, i.e., high NO but not sufficiently high to inhibit common RO₂ isomerization.

Finally, RO₂ chemistry is not only highly complex but also plays a central and instrumental role in atmospheric chemistry, in particular VOC oxidation and SOA formation. For all experiments conducted with an atmospheric chemistry simulation apparatus (chamber, flow reactor, etc.), an atmospherically relevant RO₂ chemistry is crucial to meaningful experimental results. However, most literature studies have not published experimental data that are sufficient for estimating RO₂ fate. The FIXCIT chamber experiment campaign is one of the few exceptions for which comprehensive data were reported (Nguyen et al., 2014) and used for the RO₂ fate analysis in the present work. We recommend measuring and/or estimating and reporting OH, HO₂, NO, NO₂ and OHR_{VOC} (or initial precursor composition at least) whenever possible for all future atmospheric laboratory and field experiments for organic oxidation to facilitate the analysis of RO₂ fate and the evaluation of its atmospheric relevance.

Data availability. The latest version of the general RO₂ fate estimator and OFR RO₂ Fate Estimator can be downloaded from <https://sites.google.com/site/pamwiki/hardware/estimation-equations> (last access: 17 January 2019). The model outputs in this study are available from the authors upon request (zhe.peng@colorado.edu or jose.jimenez@colorado.edu). All data shown in the figures in this paper (including the Supplement) can be downloaded from http://cires1.colorado.edu/jimenez/group_pubs.html (last access: 17 January 2019).

Appendix A: Glossary of the acronyms (except field campaign names) used in the paper.

OFR	oxidation flow reactor
VOC	volatile organic compound
SOA	secondary organic aerosol
H ₂ O	water vapor mixing ratio
OHR _{ext}	external OH reactivity (due to CO, SO ₂ , VOCs, etc.)
PAM	potential aerosol mass, a specific type of OFR
OFR185	oxidation flow reactor using both 185 and 254 nm light
OFR254	oxidation flow reactor using 254 nm light only
OFR254-X	OFR254 with X ppm O ₃ initially injected
OFR-iN ₂ O	OFR with N ₂ O initially injected
OFR185-iN ₂ O	OFR185 with N ₂ O initially injected
OFR254-iN ₂ O	OFR254 with N ₂ O initially injected
OFR254-X-iN ₂ O	OFR254-X with N ₂ O initially injected
OHR _{VOC}	OH reactivity due to VOCs
F185, F254, etc.	UV photon flux at 185 nm, 254 nm, etc.
N ₂ O	N ₂ O mixing ratio
OH _{exp} , F185 _{exp} , etc.	exposure (integral over time) to OH, F185, etc.

Appendix B: Steady-state approximation for generic RO₂

The production rate of a generic RO₂ is almost identical to the VOC consumption rate, since the second step of the conversion chain VOC → R → RO₂ is extremely fast. Therefore, the generic RO₂ production rate, P , can be expressed as follows:

$$P = \sum_i k_i c_i \cdot \text{OH} = \text{OHR}_{\text{VOC}} \cdot \text{OH}, \quad (\text{B1})$$

where OH is OH concentration and c_i and k_i are respectively the concentration and the reaction rate constant with OH of the i th VOC. OHR_{VOC} is the total OHR due to VOC and equal to $\sum_i k_i c_i$ by definition.

For the generic RO₂ loss rate, the reactions of RO₂ with HO₂, NO, RO₂, NO₂ (for acyl RO₂ only) and OH are considered. Isomerization generally does not lead to a total RO₂ concentration decrease and is thus not included in its loss rate. Then the RO₂ loss rate is

$$L = k_{\text{HO}_2} \text{RO}_2 \cdot \text{HO}_2 + k_{\text{NO}} \text{RO}_2 \cdot \text{NO} + 2k_{\text{RO}_2} \text{RO}_2 \cdot \text{RO}_2 + k_{\text{NO}_2} \text{RO}_2 \cdot \text{NO}_2 + k_{\text{OH}} \text{RO}_2 \cdot \text{OH}, \quad (\text{B2})$$

where RO₂, HO₂, NO, NO₂ and OH are the concentrations of corresponding species and k_A ($A = \text{RO}_2, \text{HO}_2, \text{NO}, \text{NO}_2$ and OH) is the reaction rate constant of RO₂ with A . For non-acyl RO₂, the term $k_{\text{NO}_2} \text{RO}_2 \cdot \text{NO}_2$ is not included; for cases with well-known pathways only (RO₂ + HO₂, RO₂ + RO₂, RO₂ + NO and RO₂ + NO₂; see Sect. 3.1), the term $k_{\text{OH}} \text{RO}_2 \cdot \text{OH}$ is excluded. k_{RO_2} needs to be given a value (which may be the main levels of RO₂ self- and cross-reaction rate constants in this study, 1×10^{-13} and 1×10^{-11} cm³ molecule⁻¹ s⁻¹, or other values depending on the RO₂ type).

At the steady state, P and L are equal. For an ambient and/or chamber setting, OH, HO₂, NO, NO₂ and OHR_{VOC} are often measured or known. In this case, simultaneously considering Eqs. (B1) and (B2) yields a quadratic equation of RO₂ concentration (the only unknown). Then the generic RO₂ concentration can be easily obtained by solving this equation:

$$\text{RO}_2 = \left(-K + \sqrt{K^2 + 8k_{\text{RO}_2} \cdot \text{OHR}_{\text{VOC}} \cdot \text{OH}} \right) / (4k_{\text{RO}_2}) \quad (\text{B3})$$

where $K = k_{\text{HO}_2} \text{HO}_2 + k_{\text{NO}} \text{NO} + k_{\text{NO}_2} \text{NO}_2 + k_{\text{OH}} \text{OH}$.

Supplement. The supplement related to this article is available online at: <https://doi.org/10.5194/acp-19-813-2019-supplement>.

Author contributions. ZP and JLJ designed the study. ZP performed most of the simulations, and JLT performed the GECKO-A simulations. JJO and GST provided advice on the organic peroxy radical chemistry. ZP, JJO, GST, and JLJ analyzed the results. ZP took the lead in writing the paper. All authors provided feedback on the paper.

Competing interests. The authors declare that they have no conflict of interest.

Acknowledgements. This work was partially supported by grants EPA STAR 83587701-0, NSF AGS-1740610, NSF AGS-1822664, NASA NNX15AT96G and DOE(BER/ASR) DE-SC0016559. We thank the following individuals for providing data from atmospheric field studies: Tran Nguyen and Jordan Krechmer (FIXCIT), William Brune (SOAS and ATom), Pedro Campuzano-Jost (ATom), Daun Jeong and Saewung Kim (GoAmazon), and Weiwei Hu (Beijing). We are also grateful to John Crounse, Joel Thornton, Paul Ziemann, Dwayne Heard, Paul Wennberg, Andrew Lambe and William Brune for useful discussions and Donna Sueper for her assistance in the development of the RO₂ Fate Estimator. NCAR is sponsored by the National Science Foundation. The EPA has not reviewed this paper and thus no endorsement should be inferred.

Edited by: Dwayne Heard

Reviewed by: two anonymous referees

References

- Assaf, E., Song, B., Tomas, A., Schoemaeker, C., and Fittschen, C.: Rate Constant of the Reaction between CH₃O₂ Radicals and OH Radicals Revisited, *J. Phys. Chem. A*, 120, 8923–8932, <https://doi.org/10.1021/acs.jpca.6b07704>, 2016.
- Assaf, E., Tanaka, S., Kajii, Y., Schoemaeker, C., and Fittschen, C.: Rate constants of the reaction of C₂–C₄ peroxy radicals with OH radicals, *Chem. Phys. Lett.*, 684, 245–249, <https://doi.org/10.1016/j.cplett.2017.06.062>, 2017a.
- Assaf, E., Sheps, L., Whalley, L., Heard, D., Tomas, A., Schoemaeker, C., and Fittschen, C.: The Reaction between CH₃O₂ and OH Radicals: Product Yields and Atmospheric Implications, *Environ. Sci. Technol.*, 51, 2170–2177, <https://doi.org/10.1021/acs.est.6b06265>, 2017b.
- Assaf, E., Schoemaeker, C., Vereecken, L., and Fittschen, C.: Experimental and theoretical investigation of the reaction of RO₂ radicals with OH radicals: Dependence of the HO₂ yield on the size of the alkyl group, *Int. J. Chem. Kinet.*, 50, 670–680, <https://doi.org/10.1002/kin.21191>, 2018.
- Atkinson, R. and Arey, J.: Atmospheric degradation of volatile organic compounds, *Chem. Rev.*, 103, 4605–4638, <https://doi.org/10.1021/cr0206420>, 2003.
- Aumont, B., Szopa, S., and Madronich, S.: Modelling the evolution of organic carbon during its gas-phase tropospheric oxidation: development of an explicit model based on a self-generating approach, *Atmos. Chem. Phys.*, 5, 2497–2517, <https://doi.org/10.5194/acp-5-2497-2005>, 2005.
- Berndt, T., Scholz, W., Mentler, B., Fischer, L., Herrmann, H., Kulmala, M., and Hansel, A.: Accretion Product Formation from Self- and Cross-Reactions of RO₂ Radicals in the Atmosphere, *Angew. Chem. Int. Edit.*, 57, 3820–3824, <https://doi.org/10.1002/anie.201710989>, 2018.
- Bossolasco, A., Faragó, E. P., Schoemaeker, C., and Fittschen, C.: Rate constant of the reaction between CH₃O₂ and OH radicals, *Chem. Phys. Lett.*, 593, 7–13, <https://doi.org/10.1016/j.cplett.2013.12.052>, 2014.
- Burkholder, J. B., Sander, S. P., Abbatt, J., Barker, J. R., Huie, R. E., Kolb, C. E., Kurylo, M. J., Orkin, V. L., Wilmouth, D. M., and Wine, P. H.: Chemical Kinetics and Photochemical Data for Use in Atmospheric Studies: Evaluation Number 18, Pasadena, CA, USA, available at: <http://jpldataeval.jpl.nasa.gov/> (last access: 30 November 2018), 2015.
- Carter, W. P. L., Cocker, D. R., Fitz, D. R., Malkina, I. L., Bumiller, K., Sauer, C. G., Pisano, J. T., Bufalino, C., and Song, C.: A new environmental chamber for evaluation of gas-phase chemical mechanisms and secondary aerosol formation, *Atmos. Environ.*, 39, 7768–7788, <https://doi.org/10.1016/j.atmosenv.2005.08.040>, 2005.
- Cocker, D. R., Flagan, R. C., and Seinfeld, J. H.: State-of-the-Art Chamber Facility for Studying Atmospheric Aerosol Chemistry, *Environ. Sci. Technol.*, 35, 2594–2601, <https://doi.org/10.1021/es0019169>, 2001.
- Crounse, J. D., Nielsen, L. B., Jørgensen, S., Kjaergaard, H. G., and Wennberg, P. O.: Autoxidation of organic compounds in the atmosphere, *J. Phys. Chem. Lett.*, 4, 3513–3520, <https://doi.org/10.1021/jz4019207>, 2013.
- D'Ambro, E. L., Møller, K. H., Lopez-Hilfiker, F. D., Schobesberger, S., Liu, J., Shilling, J. E., Lee, B. H., Kjaergaard, H. G., and Thornton, J. A.: Isomerization of Second-Generation Isoprene Peroxy Radicals: Epoxide Formation and Implications for Secondary Organic Aerosol Yields, *Environ. Sci. Technol.*, 51, 4978–4987, <https://doi.org/10.1021/acs.est.7b00460>, 2017.
- Fittschen, C., Whalley, L. K., and Heard, D. E.: The reaction of CH₃O₂ radicals with OH radicals: a neglected sink for CH₃O₂ in the remote atmosphere, *Environ. Sci. Technol.*, 48, 7700–7701, <https://doi.org/10.1021/es502481q>, 2014.
- Fry, J. L., Draper, D. C., Zarzana, K. J., Campuzano-Jost, P., Day, D. A., Jimenez, J. L., Brown, S. S., Cohen, R. C., Kaser, L., Hansel, A., Cappellin, L., Karl, T., Hodzic Roux, A., Turnipseed, A., Cantrell, C., Lefer, B. L., and Grossberg, N.: Observations of gas- and aerosol-phase organic nitrates at BEACHON-RoMBAS 2011, *Atmos. Chem. Phys.*, 13, 8585–8605, <https://doi.org/10.5194/acp-13-8585-2013>, 2013.
- Hu, W., Palm, B. B., Day, D. A., Campuzano-Jost, P., Krechmer, J. E., Peng, Z., de Sá, S. S., Martin, S. T., Alexander, M. L., Baumann, K., Hacker, L., Kiendler-Scharr, A., Koss, A. R., de Gouw, J. A., Goldstein, A. H., Seco, R., Sjostedt, S. J., Park, J.-H., Guenther, A. B., Kim, S., Canonaco, F., Prévôt, A. S. H., Brune, W. H., and Jimenez, J. L.: Volatility and lifetime against OH heterogeneous reaction of ambient isoprene-epoxydiols-derived secondary organic aerosol (IEPOX-SOA), *Atmos. Chem. Phys.*, 16, 11563–11580, <https://doi.org/10.5194/acp-16-11563-2016>, 2016.

- Huffman, J. A., Docherty, K. S., Aiken, A. C., Cubison, M. J., Ulbrich, I. M., DeCarlo, P. F., Sueper, D., Jayne, J. T., Worsnop, D. R., Ziemann, P. J., and Jimenez, J. L.: Chemically-resolved aerosol volatility measurements from two megacity field studies, *Atmos. Chem. Phys.*, 9, 7161–7182, <https://doi.org/10.5194/acp-9-7161-2009>, 2009.
- Jørgensen, S., Knap, H. C., Otkjær, R. V., Jensen, A. M., Kjeldsen, M. L. H., Wennberg, P. O., and Kjaergaard, H. G.: Rapid Hydrogen Shift Scrambling in Hydroperoxy-Substituted Organic Peroxy Radicals, *J. Phys. Chem. A*, 120, 266–275, <https://doi.org/10.1021/acs.jpca.5b06768>, 2016.
- Kalafut-Pettibone, A. J., Klems, J. P., Burgess, D. R., and McGivern, W. S.: Alkylperoxy radical photochemistry in organic aerosol formation processes, *J. Phys. Chem. A*, 117, 14141–14150, <https://doi.org/10.1021/jp4094996>, 2013.
- Kang, E., Root, M. J., Toohey, D. W., and Brune, W. H.: Introducing the concept of Potential Aerosol Mass (PAM), *Atmos. Chem. Phys.*, 7, 5727–5744, <https://doi.org/10.5194/acp-7-5727-2007>, 2007.
- Kang, E., Toohey, D. W., and Brune, W. H.: Dependence of SOA oxidation on organic aerosol mass concentration and OH exposure: experimental PAM chamber studies, *Atmos. Chem. Phys.*, 11, 1837–1852, <https://doi.org/10.5194/acp-11-1837-2011>, 2011.
- Karjalainen, P., Timonen, H., Saukko, E., Kuuluvainen, H., Saarikoski, S., Aakko-Saksa, P., Murtonen, T., Bloss, M., Dal Maso, M., Simonen, P., Ahlberg, E., Svenningsson, B., Brune, W. H., Hillamo, R., Keskinen, J., and Rönkkö, T.: Time-resolved characterization of primary particle emissions and secondary particle formation from a modern gasoline passenger car, *Atmos. Chem. Phys.*, 16, 8559–8570, <https://doi.org/10.5194/acp-16-8559-2016>, 2016.
- Klems, J. P., Lippa, K. A., and McGivern, W. S.: Quantitative Evidence for Organic Peroxy Radical Photochemistry at 254 nm, *J. Phys. Chem. A*, 119, 344–351, <https://doi.org/10.1021/jp509165x>, 2015.
- Knap, H. C. and Jørgensen, S.: Rapid Hydrogen Shift Reactions in Acyl Peroxy Radicals, *J. Phys. Chem. A*, 121, 1470–1479, <https://doi.org/10.1021/acs.jpca.6b12787>, 2017.
- Krechmer, J. E., Pagonis, D., Ziemann, P. J., and Jimenez, J. L.: Quantification of Gas-Wall Partitioning in Teflon Environmental Chambers Using Rapid Bursts of Low-Volatility Oxidized Species Generated in Situ, *Environ. Sci. Technol.*, 50, 5757–5765, <https://doi.org/10.1021/acs.est.6b00606>, 2016.
- Lambe, A., Massoli, P., Zhang, X., Canagaratna, M., Nowak, J., Daube, C., Yan, C., Nie, W., Onasch, T., Jayne, J., Kolb, C., Davidovits, P., Worsnop, D., and Brune, W.: Controlled nitric oxide production via $O(^1D) + N_2O$ reactions for use in oxidation flow reactor studies, *Atmos. Meas. Tech.*, 10, 2283–2298, <https://doi.org/10.5194/amt-10-2283-2017>, 2017.
- Lambe, A. T. and Jimenez, J. L.: PAM Wiki: User Groups, available at: <https://sites.google.com/site/pamwiki/user-groups>, last access: 2 July 2018.
- Lambe, A. T., Ahern, A. T., Williams, L. R., Slowik, J. G., Wong, J. P. S., Abbatt, J. P. D., Brune, W. H., Ng, N. L., Wright, J. P., Croasdale, D. R., Worsnop, D. R., Davidovits, P., and Onasch, T. B.: Characterization of aerosol photooxidation flow reactors: heterogeneous oxidation, secondary organic aerosol formation and cloud condensation nuclei activity measurements, *Atmos. Meas. Tech.*, 4, 445–461, <https://doi.org/10.5194/amt-4-445-2011>, 2011.
- Lambe, A. T., Cappa, C. D., Massoli, P., Onasch, T. B., Forestieri, S. D., Martin, A. T., Cummings, M. J., Croasdale, D. R., Brune, W. H., Worsnop, D. R., and Davidovits, P.: Relationship between Oxidation Level and Optical Properties of Secondary Organic Aerosol, *Environ. Sci. Technol.*, 47, 6349–6357, <https://doi.org/10.1021/es401043j>, 2013.
- Lambe, A. T., Chhabra, P. S., Onasch, T. B., Brune, W. H., Hunter, J. F., Kroll, J. H., Cummings, M. J., Brogan, J. F., Parmar, Y., Worsnop, D. R., Kolb, C. E., and Davidovits, P.: Effect of oxidant concentration, exposure time, and seed particles on secondary organic aerosol chemical composition and yield, *Atmos. Chem. Phys.*, 15, 3063–3075, <https://doi.org/10.5194/acp-15-3063-2015>, 2015.
- Levy II, H.: Normal atmosphere: large radical and formaldehyde concentrations predicted., *Science*, 173, 141–143, <https://doi.org/10.1126/science.173.3992.141>, 1971.
- Li, R., Palm, B. B., Ortega, A. M., Hu, W., Peng, Z., Day, D. A., Knote, C., Brune, W. H., de Gouw, J., and Jimenez, J. L.: Modeling the radical chemistry in an Oxidation Flow Reactor (OFR): radical formation and recycling, sensitivities, and OH exposure estimation equation, *J. Phys. Chem. A*, 119, 4418–4432, <https://doi.org/10.1021/jp509534k>, 2015.
- Lim, C. Y., Browne, E. C., Sugrue, R. A., and Kroll, J. H.: Rapid heterogeneous oxidation of organic coatings on submicron aerosols, *Geophys. Res. Lett.*, 44, 2949–2957, <https://doi.org/10.1002/2017GL072585>, 2017.
- Link, M. F., Friedman, B., Fulgham, R., Brophy, P., Galang, A., Jathar, S. H., Veres, P., Roberts, J. M., and Farmer, D. K.: Photochemical processing of diesel fuel emissions as a large secondary source of isocyanic acid (HNCO), *Geophys. Res. Lett.*, 43, 4033–4041, <https://doi.org/10.1002/2016GL068207>, 2016.
- Mao, J., Ren, X., Brune, W. H., Olson, J. R., Crawford, J. H., Fried, A., Huey, L. G., Cohen, R. C., Heikes, B., Singh, H. B., Blake, D. R., Sachse, G. W., Diskin, G. S., Hall, S. R., and Shetter, R. E.: Airborne measurement of OH reactivity during INTEX-B, *Atmos. Chem. Phys.*, 9, 163–173, <https://doi.org/10.5194/acp-9-163-2009>, 2009.
- Martin, S. T., Artaxo, P., Machado, L. A. T., Manzi, A. O., Souza, R. A. F., Schumacher, C., Wang, J., Andreae, M. O., Barbosa, H. M. J., Fan, J., Fisch, G., Goldstein, A. H., Guenther, A., Jimenez, J. L., Pöschl, U., Silva Dias, M. A., Smith, J. N., and Wendisch, M.: Introduction: Observations and Modeling of the Green Ocean Amazon (GoAmazon2014/5), *Atmos. Chem. Phys.*, 16, 4785–4797, <https://doi.org/10.5194/acp-16-4785-2016>, 2016.
- Martin, S. T., Artaxo, P., Machado, L., Manzi, A. O., Souza, R. A. F., Schumacher, C., Wang, J., Biscaro, T., Brito, J., Calheiros, A., Jardine, K., Medeiros, A., Portela, B., De Sá, S. S., Adachi, K., Aiken, A. C., Alblbrecht, R., Alexander, L., Andreae, M. O., Barbosa, H. M. J., Buseck, P., Chand, D., Comstomstock, J. M., Day, D. A., Dubey, M., Fan, J., Fastst, J., Fisch, G., Fortner, E., Giangrande, S., Gillies, M., Goldstein, A. H., Guenther, A., Hubbbbe, J., Jensen, M., Jimenez, J. L., Keuttsch, F. N., Kim, S., Kuang, C., Laskskin, A., McKinney, K., Mei, F., Milller, M., Nascimento, R., Pauliquevis, T., Pekour, M., Peres, J., Petäjä, T., Pöhklker, C., Pöschl, U., Rizzo, L., Schmid, B., Shillling, J. E., Silva Dias, M. A., Smith, J. N., Tomlinson, J. M., Tóta, J., and Wendisch, M.: The green ocean amazon experiment (GOAMA-

- ZON2014/5) observes pollution affecting gases, aerosols, clouds, and rainfall over the rain forest, *B. Am. Meteorol. Soc.*, 98, 981–997, <https://doi.org/10.1175/BAMS-D-15-00221.1>, 2017.
- Matsunaga, A. and Ziemann, P. J.: Gas-Wall Partitioning of Organic Compounds in a Teflon Film Chamber and Potential Effects on Reaction Product and Aerosol Yield Measurements, *Aerosol Sci. Tech.*, 44, 881–892, <https://doi.org/10.1080/02786826.2010.501044>, 2010.
- Müller, J.-F., Liu, Z., Nguyen, V. S., Stavrakou, T., Harvey, J. N., and Peeters, J.: The reaction of methyl peroxy and hydroxyl radicals as a major source of atmospheric methanol, *Nat. Commun.*, 7, 13213, <https://doi.org/10.1038/ncomms13213>, 2016.
- Nault, B. A., Campuzano-Jost, P., Day, D. A., Schroder, J. C., Anderson, B., Beyersdorf, A. J., Blake, D. R., Brune, W. H., Choi, Y., Corr, C. A., de Gouw, J. A., Dibb, J., DiGangi, J. P., Diskin, G. S., Fried, A., Huey, L. G., Kim, M. J., Knote, C. J., Lamb, K. D., Lee, T., Park, T., Pusede, S. E., Scheuer, E., Thornhill, K. L., Woo, J.-H., and Jimenez, J. L.: Secondary organic aerosol production from local emissions dominates the organic aerosol budget over Seoul, South Korea, during KORUS-AQ, *Atmos. Chem. Phys.*, 18, 17769–17800, <https://doi.org/10.5194/acp-18-17769-2018>, 2018.
- Nel, A.: Air Pollution-Related Illness: Effects of Particles, *Science*, 308, 804–806, <https://doi.org/10.1126/science.1108752>, 2005.
- Nguyen, T. B., Crounse, J. D., Schwantes, R. H., Teng, A. P., Bates, K. H., Zhang, X., St. Clair, J. M., Brune, W. H., Tyndall, G. S., Keutsch, F. N., Seinfeld, J. H., and Wennberg, P. O.: Overview of the Focused Isoprene eXperiment at the California Institute of Technology (FIXCIT): mechanistic chamber studies on the oxidation of biogenic compounds, *Atmos. Chem. Phys.*, 14, 13531–13549, <https://doi.org/10.5194/acp-14-13531-2014>, 2014.
- Orlando, J. J. and Tyndall, G. S.: Laboratory studies of organic peroxy radical chemistry: an overview with emphasis on recent issues of atmospheric significance, *Chem. Soc. Rev.*, 41, 6294–6317, <https://doi.org/10.1039/c2cs35166h>, 2012.
- Ortega, A. M., Day, D. A., Cubison, M. J., Brune, W. H., Bon, D., de Gouw, J. A., and Jimenez, J. L.: Secondary organic aerosol formation and primary organic aerosol oxidation from biomass-burning smoke in a flow reactor during FLAME-3, *Atmos. Chem. Phys.*, 13, 11551–11571, <https://doi.org/10.5194/acp-13-11551-2013>, 2013.
- Ortega, A. M., Hayes, P. L., Peng, Z., Palm, B. B., Hu, W., Day, D. A., Li, R., Cubison, M. J., Brune, W. H., Graus, M., Warneke, C., Gilman, J. B., Kuster, W. C., de Gouw, J., Gutiérrez-Montes, C., and Jimenez, J. L.: Real-time measurements of secondary organic aerosol formation and aging from ambient air in an oxidation flow reactor in the Los Angeles area, *Atmos. Chem. Phys.*, 16, 7411–7433, <https://doi.org/10.5194/acp-16-7411-2016>, 2016.
- Ortega, J., Turnipseed, A., Guenther, A. B., Karl, T. G., Day, D. A., Gochis, D., Huffman, J. A., Prenni, A. J., Levin, E. J. T., Kreidenweis, S. M., DeMott, P. J., Tobo, Y., Patton, E. G., Hodzic, A., Cui, Y. Y., Harley, P. C., Hornbrook, R. S., Apel, E. C., Monson, R. K., Eller, A. S. D., Greenberg, J. P., Barth, M. C., Campuzano-Jost, P., Palm, B. B., Jimenez, J. L., Aiken, A. C., Dubey, M. K., Geron, C., Offenberg, J., Ryan, M. G., Fornwalt, P. J., Pryor, S. C., Keutsch, F. N., DiGangi, J. P., Chan, A. W. H., Goldstein, A. H., Wolfe, G. M., Kim, S., Kaser, L., Schnitzhofer, R., Hansel, A., Cantrell, C. A., Mauldin, R. L., and Smith, J. N.: Overview of the Manitou Experimental Forest Observatory: site description and selected science results from 2008 to 2013, *Atmos. Chem. Phys.*, 14, 6345–6367, <https://doi.org/10.5194/acp-14-6345-2014>, 2014.
- Palm, B. B., Campuzano-Jost, P., Ortega, A. M., Day, D. A., Kaser, L., Jud, W., Karl, T., Hansel, A., Hunter, J. F., Cross, E. S., Kroll, J. H., Peng, Z., Brune, W. H., and Jimenez, J. L.: In situ secondary organic aerosol formation from ambient pine forest air using an oxidation flow reactor, *Atmos. Chem. Phys.*, 16, 2943–2970, <https://doi.org/10.5194/acp-16-2943-2016>, 2016.
- Palm, B. B., Campuzano-Jost, P., Day, D. A., Ortega, A. M., Fry, J. L., Brown, S. S., Zarzana, K. J., Dube, W., Wagner, N. L., Draper, D. C., Kaser, L., Jud, W., Karl, T., Hansel, A., Gutiérrez-Montes, C., and Jimenez, J. L.: Secondary organic aerosol formation from in situ OH, O₃, and NO₃ oxidation of ambient forest air in an oxidation flow reactor, *Atmos. Chem. Phys.*, 17, 5331–5354, <https://doi.org/10.5194/acp-17-5331-2017>, 2017.
- Peng, Z. and Jimenez, J. L.: Modeling of the chemistry in oxidation flow reactors with high initial NO, *Atmos. Chem. Phys.*, 17, 11991–12010, <https://doi.org/10.5194/acp-17-11991-2017>, 2017.
- Peng, Z., Day, D. A., Stark, H., Li, R., Lee-Taylor, J., Palm, B. B., Brune, W. H., and Jimenez, J. L.: HO_x radical chemistry in oxidation flow reactors with low-pressure mercury lamps systematically examined by modeling, *Atmos. Meas. Tech.*, 8, 4863–4890, <https://doi.org/10.5194/amt-8-4863-2015>, 2015.
- Peng, Z., Day, D. A., Ortega, A. M., Palm, B. B., Hu, W., Stark, H., Li, R., Tsigaridis, K., Brune, W. H., and Jimenez, J. L.: Non-OH chemistry in oxidation flow reactors for the study of atmospheric chemistry systematically examined by modeling, *Atmos. Chem. Phys.*, 16, 4283–4305, <https://doi.org/10.5194/acp-16-4283-2016>, 2016.
- Peng, Z., Palm, B. B., Day, D. A., Talukdar, R. K., Hu, W., Lambe, A. T., Brune, W. H., and Jimenez, J. L.: Model Evaluation of New Techniques for Maintaining High-NO Conditions in Oxidation Flow Reactors for the Study of OH-Initiated Atmospheric Chemistry, *ACS Earth Sp. Chem.*, 2, 72–86, <https://doi.org/10.1021/acsearthspacechem.7b00070>, 2018.
- Platt, S. M., El Haddad, I., Zardini, A. A., Clairotte, M., Astorga, C., Wolf, R., Slowik, J. G., Temime-Roussel, B., Marchand, N., Ježek, I., Drinovec, L., Mocnik, G., Möhler, O., Richter, R., Barmet, P., Bianchi, F., Baltensperger, U., and Prévôt, A. S. H.: Secondary organic aerosol formation from gasoline vehicle emissions in a new mobile environmental reaction chamber, *Atmos. Chem. Phys.*, 13, 9141–9158, <https://doi.org/10.5194/acp-13-9141-2013>, 2013.
- Praske, E., Otkjær, R. V., Crounse, J. D., Hethcox, J. C., Stoltz, B. M., Kjaergaard, H. G., and Wennberg, P. O.: Atmospheric autoxidation is increasingly important in urban and suburban North America, *P. Natl. Acad. Sci. USA*, 115, 64–69, <https://doi.org/10.1073/pnas.1715540115>, 2018.
- Presto, A. A., Huff Hartz, K. E., and Donahue, N. M.: Secondary Organic Aerosol Production from Terpene Ozonolysis. 1. Effect of UV Radiation, *Environ. Sci. Technol.*, 39, 7036–7045, <https://doi.org/10.1021/es050174m>, 2005.
- Richards-Henderson, N. K., Goldstein, A. H., and Wilson, K. R.: Large Enhancement in the Heterogeneous Oxidation Rate of Organic Aerosols by Hydroxyl Radicals in the Pres-

- ence of Nitric Oxide, *J. Phys. Chem. Lett.*, 6, 4451–4455, <https://doi.org/10.1021/acs.jpcllett.5b02121>, 2015.
- Richards-Henderson, N. K., Goldstein, A. H., and Wilson, K. R.: Sulfur Dioxide Accelerates the Heterogeneous Oxidation Rate of Organic Aerosol by Hydroxyl Radicals, *Environ. Sci. Technol.*, 50, 3554–3561, <https://doi.org/10.1021/acs.est.5b05369>, 2016.
- Ryerson, T. B., Andrews, A. E., Angevine, W. M., Bates, T. S., Brock, C. A., Cairns, B., Cohen, R. C., Cooper, O. R., De Gouw, J. A., Fehsenfeld, F. C., Ferrare, R. A., Fischer, M. L., Flagan, R. C., Goldstein, A. H., Hair, J. W., Hardesty, R. M., Hostetler, C. A., Jimenez, J. L., Langford, A. O., McCauley, E., McKeen, S. A., Molina, L. T., Nenes, A., Oltmans, S. J., Parrish, D. D., Pederson, J. R., Pierce, R. B., Prather, K., Quinn, P. K., Seinfeld, J. H., Senff, C. J., Sorooshian, A., Stutz, J., Surratt, J. D., Trainer, M., Volkamer, R., Williams, E. J., and Wofsy, S. C.: The 2010 California Research at the Nexus of Air Quality and Climate Change (CalNex) field study, *J. Geophys. Res.-Atmos.*, 118, 5830–5866, <https://doi.org/10.1002/jgrd.50331>, 2013.
- Stocker, T. F., Qin, D., Plattner, G.-K., Tignor, M., Allen, S. K., Boschung, J., Nauels, A., Xia, Y., Bex, V., and Midgley, P. M.: *Climate Change 2013 – The Physical Science Basis*, edited by Intergovernmental Panel on Climate Change, Cambridge University Press, Cambridge, 2014.
- Stone, D., Whalley, L. K., and Heard, D. E.: Tropospheric OH and HO₂ radicals: field measurements and model comparisons, *Chem. Soc. Rev.*, 41, 6348–6404, <https://doi.org/10.1039/c2cs35140d>, 2012.
- Tkacik, D. S., Lambe, A. T., Jathar, S., Li, X., Presto, A. A., Zhao, Y., Blake, D., Meinardi, S., Jayne, J. T., Croteau, P. L., and Robinson, A. L.: Secondary Organic Aerosol Formation from in-Use Motor Vehicle Emissions Using a Potential Aerosol Mass Reactor, *Environ. Sci. Technol.*, 48, 11235–11242, <https://doi.org/10.1021/es502239v>, 2014.
- Wang, J., Doussin, J. F., Perrier, S., Perraudin, E., Katrib, Y., Pan-gui, E., and Picquet-Varrault, B.: Design of a new multi-phase experimental simulation chamber for atmospheric photochem, aerosol and cloud chemistry research, *Atmos. Meas. Tech.*, 4, 2465–2494, <https://doi.org/10.5194/amt-4-2465-2011>, 2011.
- Wofsy, S. C., Apel, E., Blake, D. R., Brock, C. A., Brune, W. H., Bui, T. P., Daube, B. C., Dibb, J. E., Diskin, G. S., Elkins, J. W., Froyd, K., Hall, S. R., Hanisco, T. F., Huey, L. G., Jimenez, J. L., McKain, K., Montzka, S. A., Ryerson, T. B., Schwarz, J. P., Stephens, B. B., Weinzierl, B., and Wennberg, P.: *ATom: Merged Atmospheric Chemistry, Trace Gases, and Aerosols*, Oak Ridge, Tennessee, USA, 2018.
- Yan, C., Kocovska, S., and Krasnoperov, L. N.: Kinetics of the Reaction of CH₃O₂ Radicals with OH Studied over the 292–526 K Temperature Range, *J. Phys. Chem. A*, 120, 6111–6121, <https://doi.org/10.1021/acs.jpca.6b04213>, 2016.
- Zhang, X., Cappa, C. D., Jathar, S. H., McVay, R. C., Ensberg, J. J., Kleeman, M. J., and Seinfeld, J. H.: Influence of vapor wall loss in laboratory chambers on yields of secondary organic aerosol, *P. Natl. Acad. Sci. USA*, 111, 5802–5807, <https://doi.org/10.1073/pnas.1404727111>, 2014.
- Ziemann, P. J. and Atkinson, R.: Kinetics, products, and mechanisms of secondary organic aerosol formation, *Chem. Soc. Rev.*, 41, 6582–6605, <https://doi.org/10.1039/c2cs35122f>, 2012.